

Review

Metal and Metal Oxide Nanoparticles Catalyzed C–H Activation for C–O and C–X (X = Halogen, B, P, S, Se) Bond Formation

Federica Valentini, Oriana Piermatti *  and Luigi Vaccaro * 

Laboratory of Green S.O.C., Dipartimento di Chimica, Biologia e Biotecnologie, Università degli Studi di Perugia, Via Elce di Sotto 8, 06123 Perugia, Italy

* Correspondence: oriana.piermatti@unipg.it (O.P.); luigi.vaccaro@unipg.it (L.V.)

Abstract: The direct functionalization of an inactivated C–H bond has become an attractive approach to evolve toward step-economy, atom-efficient and environmentally sustainable processes. In this regard, the design and preparation of highly active metal nanoparticles as efficient catalysts for C–H bond activation under mild reaction conditions still continue to be investigated. This review focuses on the functionalization of un-activated C(sp³)–H, C(sp²)–H and C(sp)–H bonds exploiting metal and metal oxide nanoparticles C–H activation for C–O and C–X (X = Halogen, B, P, S, Se) bond formation, resulting in more sustainable access to industrial production.

Keywords: metal nanoparticles; metal oxide nanoparticles; C–H activation; C–O bond formation; C–X bond formation



Citation: Valentini, F.; Piermatti, O.; Vaccaro, L. Metal and Metal Oxide Nanoparticles Catalyzed C–H Activation for C–O and C–X (X = Halogen, B, P, S, Se) Bond Formation. *Catalysts* **2023**, *13*, 16. <https://doi.org/10.3390/catal13010016>

Academic Editor: Mauro Bassetti

Received: 17 November 2022

Revised: 15 December 2022

Accepted: 19 December 2022

Published: 22 December 2022



Copyright: © 2022 by the authors. Licensee MDPI, Basel, Switzerland. This article is an open access article distributed under the terms and conditions of the Creative Commons Attribution (CC BY) license (<https://creativecommons.org/licenses/by/4.0/>).

1. Introduction

The direct and selective introduction of a new functionality via direct C–H bond activation has become a highly attractive strategy for the preparation of valuable target compounds. The direct activation of relatively inert C–H bonds allows avoiding additional pre-functionalization steps, minimizing the number of synthetic transformations and resulting in protocols with higher atom economy sustainability [1–4].

However, due to the ubiquitous presence of C–H bonds and their high bond dissociation energy, the development of efficient catalysts is essential, aiming for their activation using mild conditions and with a good control of selectivity.

A large number of homogeneous metal complexes, mainly group VIII (Ru, Rh, Pt, Ir, Pd and Co), have proven to be efficiently able to coordinate a C–H bond and can be successfully used for C–H activation/functionalization processes [5–21]. These catalysts are often toxic and expensive, and their use often leads to a difficult separation from the products that remain contaminated; their recovery and reuse is also difficult if not impossible.

In the past two decades, metal nanoparticles (MNPs) have found successful use as catalytic systems to promote a wide range of transformations such as C–C coupling, reduction and oxidation reactions [22–30]. More recently, due to their tunable electronic, chemical properties, shape, size and composition, MNPs with a high surface-to-volume ratio have been shown to be very efficient catalyst for the C–H functionalization (C–C, C–Heteroatom) via C–H activation under mild reaction conditions [31–50].

As is well-established, nanoparticle size and shape, stabilizing ligand, nature of support and reaction conditions (such as temperature, reaction medium and the nature of reagents) play a key role in the fine tuning of the efficiency of nanocatalyst. MNPs may either exhibit surface reactivity with a more heterogeneous catalytic mechanism or generate soluble active molecular species, leading to homogeneous catalytic behavior (release and catch mechanism). The different mechanism of action, combined with the proper choice of reaction medium and conditions, has an inevitably strong impact on the recoverability/reusability of the catalytic system [51,52].

Nanocatalysis is emerging as a powerful tool in organic synthesis for the construction of synthetically relevant building blocks via C–H activation. Among the different transformations, the formation of new C–heteroatoms bonds is usually less investigated and discussed. To fill this gap in this review, we will focus on the analysis of literature concerning the use of metal and metal oxide nanoparticles to promote the activation of C(sp³)–H, C(sp²)–H and C(sp)–H bonds for the formation of new C–heteroatom bonds. We classified the examples reported based on the bonds formed, C–O, C–halogen, C–B, C–P, C–S or C–Se.

2. Carbon-Oxygen (C–O) Bond Formation

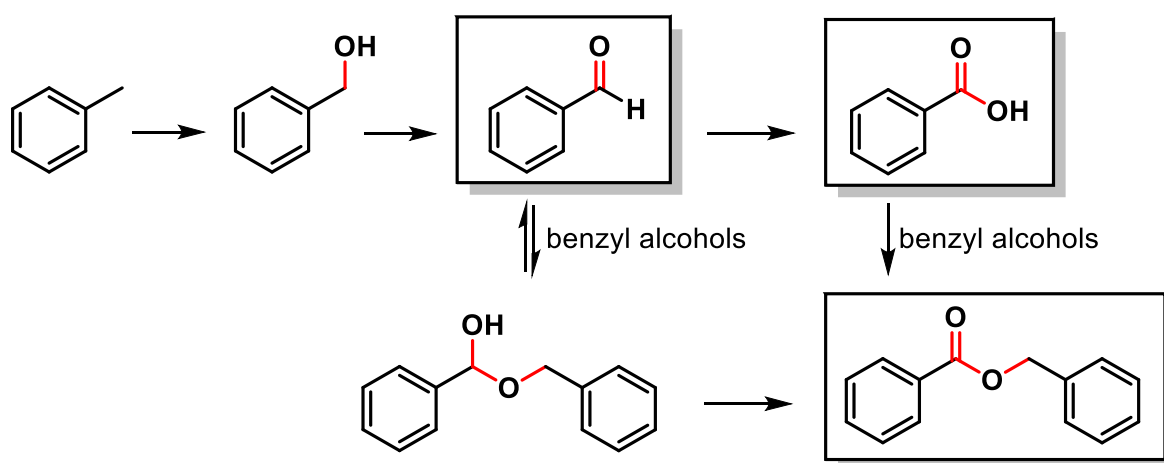
Various noble metal and nonprecious metal or metal oxide nanoparticles have been utilized to exploit the C–H activation process to promote the formation of a new C–O bond and access alcohols or carbonyls. The relevance of this method relies in the importance of these products as key intermediates for the production of fine chemicals and pharmaceuticals, as well as agrochemicals [53–56].

Among these processes, it is worthwhile to mention the representative selective oxidation of methane that remains a chemical challenge due to large energy barriers and the prevention of overoxidation to CO₂ [36,57–59]. Generally, high temperatures are required, but relatively mild conditions have been recently obtained by using bimetallic systems, such as AuPd NPs [60]. Moreover, methane can form stable adducts with alkaline metal cations in the gas phase [61]. In this review, we will focus on C(sp³) and the C(sp²)–H activation of alkanes, arenes and alkenes.

2.1. Toluene C(sp³)–H Activation

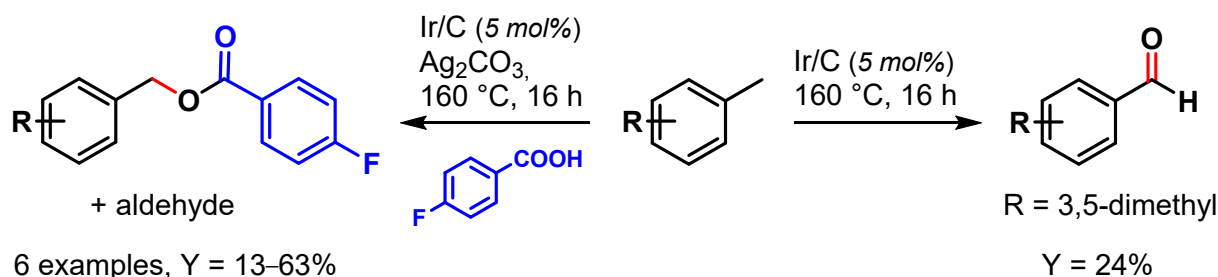
The selective C–H oxidation of toluene using MNPs has been widely explored [57]. Generally, high temperature and high O₂ pressure are required, often leading to a poor control of selectivity. Therefore, the search for an efficient catalyst exhibiting high activity and selectivity under mild conditions still represents a challenge.

The C–H oxidation of toluene can lead to the formation of benzyl alcohol, benzaldehyde, benzoic acid or benzyl benzoate (Scheme 1).



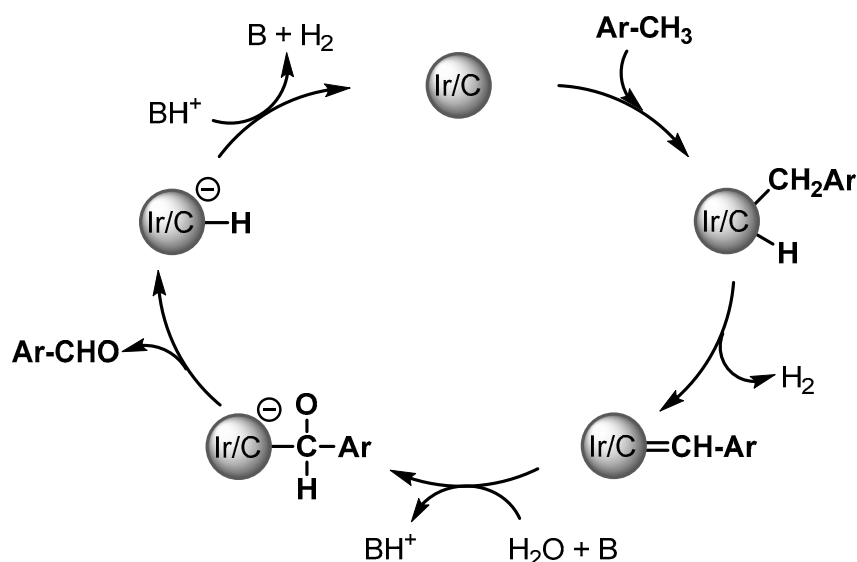
Scheme 1. C(sp³)–H oxidation of toluene.

In 2009, Crabtree and coworkers [62] showed the use of a recyclable Ir/C catalyst in the selective oxidation of toluene and its derivatives. When the reaction was performed in the presence of Ag₂CO₃, acting both as base and oxidant, benzyl alcohol was observed as major product, which, forming in the presence of 4-fluorobenzoic acid, gave the corresponding ester and aldehyde as side products. In the absence of Ag₂CO₃, aldehydes were obtained exclusively (Scheme 2).



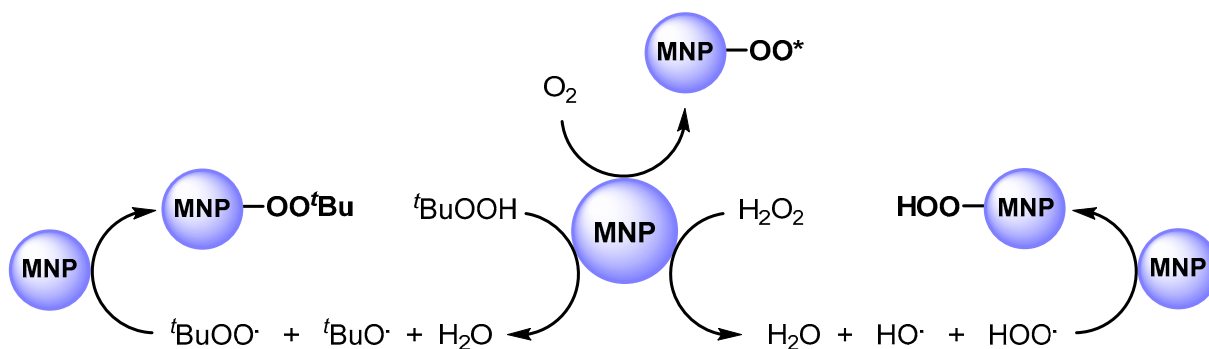
Scheme 2. Ir/C catalyzed C–H oxidation of toluene.

Aldehydes are formed via a double gem C–H activation of ArCH_3 , possibly forming a surface-bound $\text{ArCH} = \text{Schrock carbene}$. Then water provides the oxygen source for C–O bond formation and α -hydride elimination, followed by the reductive elimination of the product leading to the formation of the aldehydes (Scheme 3).



Scheme 3. Plausible mechanism of Ir/C catalyzed aldehyde formation.

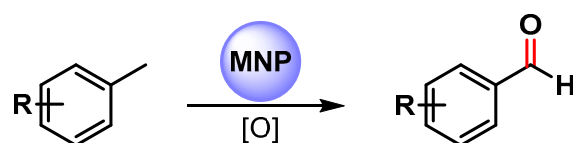
In 2011, Hutchings and coworkers [63] studied the catalytic activity of AuPd alloy NPs, prepared by sol-gel immobilization on carbon (Au-Pd/C). They used this catalytic system in the solvent free C–H bond oxidation of toluene at 160 °C in the presence of O_2 (10 bar) and obtained benzyl benzoate with high yield and selectivity. It was found that metal nanoparticles significantly enhanced oxygen adsorption and are able to promote the formation of a surface-active superoxide species, such as $\text{O}_2^{\cdot-}$, and $\text{O}_2^{\cdot-}$ (O_2^*), that promote C–H abstraction (Scheme 4).



Scheme 4. Formation of surface-bound oxygen radical species.

In 2012, the same authors [64] performed the C–H oxidation of toluene in milder conditions, at 80 °C, by using Au-Pd nanoparticles immobilized on TiO₂ (Au-Pd/TiO₂) in the presence of *tert*-butyl hydroperoxide (TBHP). The authors showed, for the first time, that MNPs can efficiently promote the decomposition of peroxides such as TBHP (or H₂O₂) to generate the *tert*-butyl peroxy (t-BuOO·) and *tert*-butoxy (t-BuO·) radical species (i.e., hydroperoxy and hydroxy radical species). The obtained radicals can be adsorbed on the surface of the metal to generate surface-bound radical species that play a key role in C–H bond activation (Scheme 4).

More recently, a wide variety of metal and metal oxide nanoparticles have been used for the selective oxidation of toluene via C–H activation, and examples of the selective formation of benzaldehyde are listed in Scheme 5 [65–69].



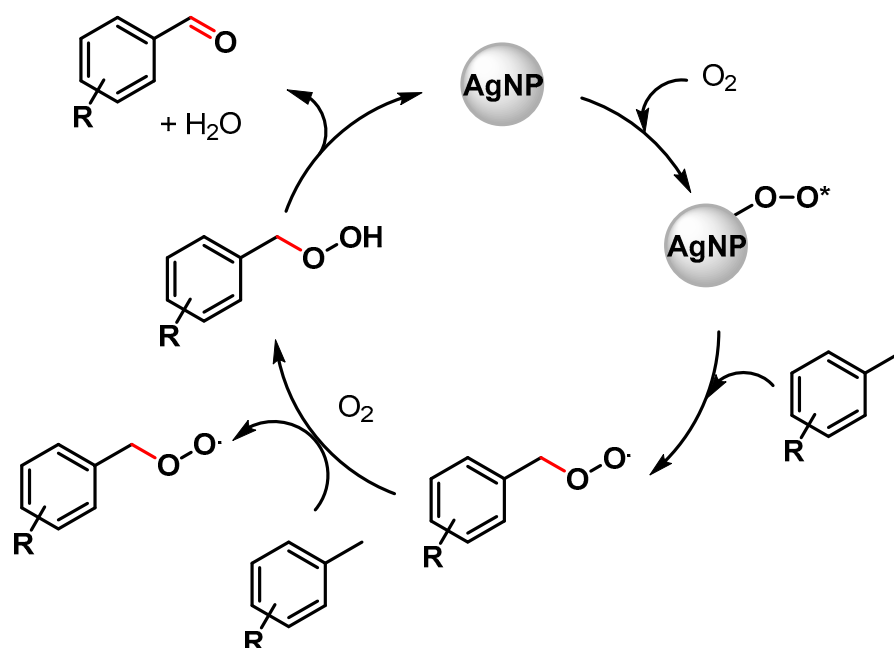
● CdO ₂ or ZnO ₂ (2 mol%)	160–180 °C	R = H
● In ₂ O ₃ -TUD-1 (100 mg/8 mmol)	[TBHP, 80 °C], CH ₃ COOH	R = H
● Ag-TESPTS@SBA-15 (12 mol%)	[O ₂ , 110 °C]	11 examples
● Cs ₃ Bi ₂ Cr ₉ /SBA-15 (10 mg/5 ml)	[air, 293 °K, hv]	5 examples
● Cs ₃ Sb ₂ Br ₉ (10 mg/5 ml)	[O ₂ , 293 °K, hv]	3 examples

Scheme 5. C(sp³)–H bond activation of toluene to benzaldehyde.

In 2013, Rao and coworkers [65] reported the C–H bond activation of toluene by using metal peroxide nanoparticles, CdO₂ and ZnO₂, prepared by a reaction of the corresponding oxide with H₂O₂. These metal peroxides are able to oxidize toluene primarily to benzaldehyde in the range of 160–180 °C. At this temperature, the peroxide nanoparticles decompose to give the corresponding oxides. Although CdO₂ nanoparticles showed higher yields, more environmentally benign ZnO₂ is better in terms of selectivity. A benzyl hydroperoxide intermediate has been detected during the transformation of toluene to benzaldehyde.

In 2020, Das and Chowdhury [66] described the use of indium oxide nanoparticles embedded in mesoporous silica TUD-1 (In-TUD-1) for the green synthesis of benzaldehyde from toluene using TBHP as oxygen donor and acetic acid as solvent, under very mild reaction conditions (80 °C, 5 h). The catalyst showed high catalytic activity with 48% toluene conversion and 83% benzaldehyde selectivity. Moreover, the catalyst was recyclable up to five times (from 48 to 36%). The use of a radical scavenger, such as quinhydrone, stopped the reaction, suggesting that it proceeds through a radical chain mechanism. The coordination of TBHP on the surface of In₂O₃ generates the *tert*-butyl peroxy (t-BuOO·) and *tert*-butoxy (t-BuO·) radical species. Toluene reacted with surface radical species to form the benzyl radical that combined with the metal surface and *tert*-butyl peroxy radical to produce benzaldehyde and *t*-BuOH as a by-product.

In the same year, Biswas and coworkers [67] described the preparation of highly dispersed silver nanoparticles supported on 2D hexagonally ordered functionalized mesoporous silica (Ag-TESPTS@SBA-15, AgMS) and their catalytic application in the C–H activation of toluene and its derivatives to produce the corresponding aldehydes under solvent-free conditions using a flow of oxygen at 110 °C. Moderate to good yields (59–79%) and high selectivities (89–96%) were achieved with both electron-rich and electron-poor groups. A significant decrease in the reaction yield was observed in the presence of TEMPO, confirming a radical pathway for the C–H oxidation wherein AgNPs promote the activation of O₂ molecules with the formation on the surface of active oxygen species and of a benzyl peroxy radical intermediate (Scheme 6).



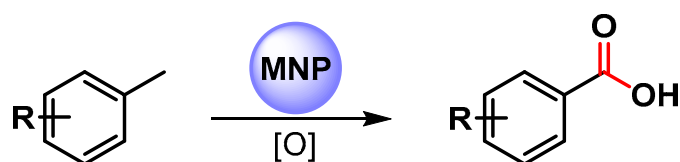
Scheme 6. Proposed mechanism for C(sp³)-H bond activation of toluene with AgNPs.

In 2020, Cs₃Bi₂Br₉ perovskite nanoparticles immobilized in the pore channels of mesoporous silica SBA-15 were used as a photocatalyst in the C-H activation of toluene and its derivatives by Tgygsgz and coworkers [68]. The reactions were performed under visible-light irradiation (>420 nm) in air at 293 K, obtaining the corresponding aldehydes with a high conversion rate and selectivity (80–90%). A control experiment with TEMPO and TEMPO-H verified the formation of a carbon-centered radical as an intermediate, and isotopic labeling experiments ($K_H/K_D = 4.4$) showed that the C(sp³)-H bond activation was the rate-determining step.

Similarly, in the same year, Xu and coworkers [69] reported the use of Cs₃Sb₂Br₉ perovskite nanoparticles as a photocatalyst under visible-light irradiation (>420 nm), in an O₂ atmosphere at 293 K for the oxidation of toluene to benzaldehyde.

In a recent paper, Fan and coworkers [70] described the selective oxidation of benzyl alcohol to benzaldehyde via C-H activation under solvent-free conditions at 120 °C. The protocol implies the use of O₂ as oxidant and electron-rich Pd atoms consisting of AuPd bimetallic NPs immobilized on TiO₂ as catalyst. Extremely high turnover frequency was observed for AuPd_x/TiO₂ with $x = 0.001$. Moreover, kinetic studies reveal that the electron rich Pd atoms accelerate the oxidation of benzyl alcohols compared to net Pd atoms and that the cleavage of C-H bond is the rate-determining step ($K_H/K_D = 11.34$).

Very few examples deal with the use of MNPs as a catalyst for the selective C-H oxidation of toluene to benzoic acid (Scheme 7) [71–73].



- | | | |
|-----------------------------|--|-------------|
| ● Au-pDA-rGO (0.2 mol%) | [O ₂ , 60 °C], CH ₃ CN | R = H |
| ● Mn/Co-ZNC (30 mg/28 mmol) | [TBHP, O ₂ , 120 °C] | 11 examples |
| ● Cu@AEPOP (8 mol%) | [TBHP, 70 °C] | R = H |

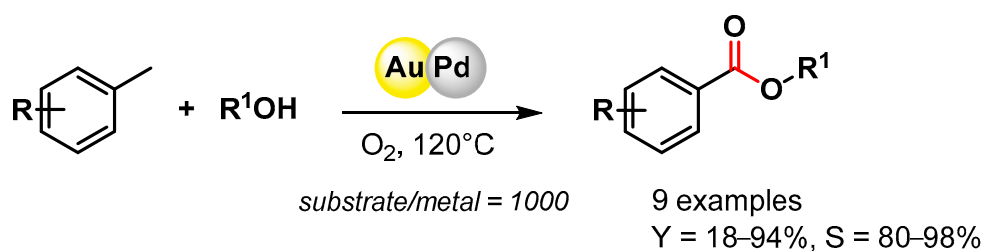
Scheme 7. C(sp³)-H bond activation of toluene to benzoic acid.

In 2016, Sama and coworkers [71] reported the preparation of Au NPs supported on polydopamine-reduced graphene oxide (Au-pDA-rGO) and its use as catalyst for the selective oxidation of benzylic C–H bonds in CH₃CN at 60 °C under an O₂ atmosphere (10 bar) in the presence of *N*-hydroxyphthalimide (NHPI). Benzoic acid was obtained with good conversion (60%) and very high selectivity (99.6%). Detailed mechanistic studies showed that the reaction followed a free radical pathway in which O₂ activation takes place on AuNPs' surfaces, generating a superoxide species that, in the presence of NHPI, generates a phthalimide *N*-oxyl radical (PINO) responsible for C–H breaking to generate benzyl radicals.

In 2021, bimetallic Mn/Co oxide nanoparticles confined in zeolite imidazolate frameworks (ZIFs) were described by Huang and coworkers [72]. The C–H oxidation of toluene and substituted toluenes to corresponding carboxylic acids were performed at 120 °C, in the presence of O₂ (6 bar) and TBHP as oxidants. Moderate to good conversion rates (39–57%) were obtained with high selectivity (up to 98.6%). A controlled experiment with TEMPO indicates a radical mechanism in which the activation of O₂ by metal oxide generate the superoxide radical species that react with TBHP, generating *tert*-butyl peroxide species responsible for C–H activation by chain-propagating steps. Moreover, the catalyst was recovered and reused for six replicate runs with conversion and selectivity almost unchanged (from 57 to 43% conversion, up to 98% selectivity). A slight drop in reactivity and selectivity were observed thereafter.

In 2022, Wang and coworkers [73] reported the use of a porous organic polymer immobilized copper nanoparticles (Cu@AEPOP) as an efficient catalyst for benzylic C–H bond oxidation. Toluene oxidation to benzoic acid was easily performed at 70 °C in the presence of 70% in water TBHP as the sole oxidant (90% yield). A radical mechanism was hypothesized in which TBHP decomposes on the surface of Cu NPs to give the *t*-BuO• and *t*-BuOO• radical species responsible for benzylic hydrogen abstraction.

The direct oxidative esterification of methyl arenes with alcohols was reported by Liu and coworker in 2012 [74]. Bimetallic AuPd NPs supported on a metal–organic framework (MIL-101) promoted C–H activation at 120 °C in the presence of O₂, producing the corresponding esters with good yields and high selectivities (Scheme 8). The catalyst was recovered and reused for 3 runs without a significant loss of catalytic activity (from 34.3 to 35.2% conversion and from 87.8 to 88.5% selectivity).



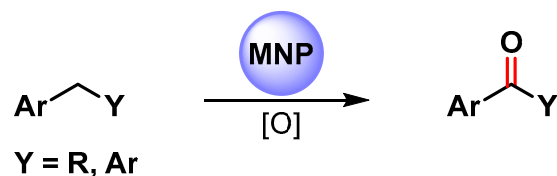
Scheme 8. Direct oxidative esterification of methyl arenes in presence of AuPd/MIL-101.

In 2018, Varma and coworkers [75] synthesized graphitic-carbon-nitride-supported palladium nanoparticles (Pd@g-C₃N₄) for the photocatalytic C–H activation of benzyl alcohols to methyl esters with high yield and selectivity by using visible-light irradiation, under air, at room temperature (91–96% isolated yield). The photocatalyst was recycled and reused up to five times without losing its activity (from 96 to 95% yield) and with negligible Pd leaching.

An oxidative esterification of benzaldehyde via C–H activation at room temperature, using visible-light irradiation and Ag/Co₃O₄ supported on a reduced graphene oxide (rGO) nanocomposite in the presence of alcohol as solvent was reported by Zhang in 2020 [76]. High conversion (72–90%) and selectivity (up to 99%) were obtained with a wide variety of alcohols (ROH, R = Me, Et, Pr, *i*Pr, Bu).

2.2. Alkyl Arenes C(sp³)-H Activation

The catalyzed oxidative C–H activation of alkyl arenes is a chemical process to obtain aromatic ketones directly. Recently, a large number of metal and metal oxide nanoparticles that efficiently promote oxidative C–H functionalization in mild conditions have been widely developed (Scheme 9) [67,71,73,77–80].



● Au-pDA-rGO (0.2 mol%)	[O ₂ , 60 °C], CH ₃ CN	9 examples
● Pt@Bi ₂ MoO ₆ (2,4 mol%)	[O ₂ , 17 °C, hv], C ₆ H ₅ CF ₃	9 examples
● Ag-TESPTS@SBA-15 (12 mol%)	[O ₂ , 110 °C]	11 examples
● CuO/N-C-HNSs (20 wt%)	[TBHP, 80 °C]	8 examples
● LaMnO ₃ (100mg/0.5 mmol)	[O ₂ , 80 °C], eptane	3 examples
● Mg ₆ MnO ₈ (100 mg/0.5 mmol)	[O ₂ , 50 °C], octane	16 examples
● Cu@AEPOP (4 mol%)	[TBHP, 70 °C]	10 examples

Scheme 9. C(sp³)-H bond oxidation of alkylarenes to ketones.

The Au-NPs-based catalyst (Au-pDA-rGO) used by Sama and coworker in the selective oxidation of toluene to benzoic acid was also used for the selective benzylic C–H bond activation of alkyl arenes to the corresponding ketones [71]. The Au nanocomposite under an O₂ atmosphere (10 bar) in the presence of N-hydroxyphthalimide (NHPI) leads to the desired oxidation products under mild and neutral reaction conditions with high efficiency and selectivity (80–99.5% conversion, up to 98.8% selectivity).

In 2018, Cheng and coworkers [77] reported a selective oxidation of alkyl aromatics under visible-light irradiation, at 17 °C in CF₃C₆H₅, using O₂ as an oxidant and Pt NPs supported on Bi₂MoO₆ semiconductor nanoplates as the photocatalyst. Generally, ketone was obtained as the main product, but for a number of substrates, alcohol was also observed. Under visible-light irradiation, the Bi₂MoO₆ nanoplates produce photogenerated holes and electrons: the holes oxidize the alkyl aromatic and form the radical cation, while the photogenerated electrons transfer to Pt NPs. Pt nanoparticles, as cocatalysts, suppress the recombination of a photogenerated charge, promote oxygen reduction and activate the benzylic C–H bonds. The stability of Pt/Bi₂MoO₆ nanoplates was investigated in a cycling experiment, and no significant activity loss was observed after six consecutive runs (from 90 to 87% conversion).

The Ag-TESPTS@SBA-15 catalyst [67], reported by Biswas and coworkers for the selective oxidation of toluene derivatives to the corresponding aldehyde, was also employed in the oxidative C–H bond activation of alkyl aromatics, under eco-friendly reaction conditions, to produce the corresponding ketones. The reactions exhibit good yields (59–80%) and excellent selectivities (91–94%) toward the formation of carbonyl compounds, and very good TON and TOF were also obtained.

Highly active CuO nanoparticles supported on nitrogen-doped carbon hollow nanospheres (CuO/N-CHNSs) were obtained by Kantam and coworkers in 2021 [78]. The catalyst was efficiently used in the selective C(sp³)-H bond oxidation of alkyl aromatics to corresponding ketones under mild conditions by using TBHP as the oxidant and water as the green solvent at 80 °C. High conversion and selectivity (up to 99%) were obtained for a wide range of aromatic hydrocarbons. Moreover, the catalyst was easily recovered and reused for up to 5 runs without a significant decrease of catalytic activity (from 98 to 92% yield). The high catalytic activity and reusability was attributed to the

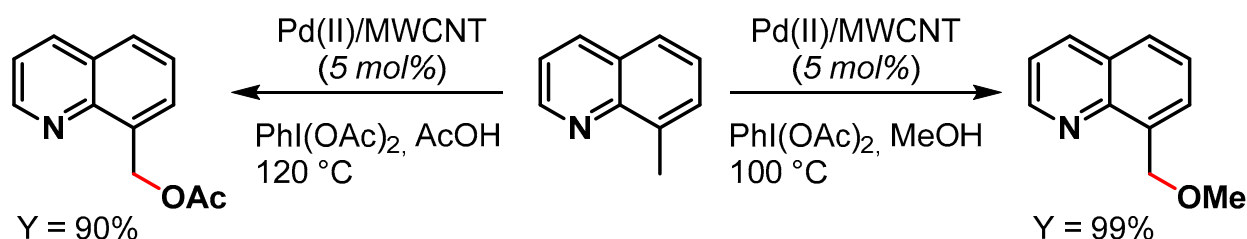
synergistic effect between finely dispersed CuO nanoparticles and nitrogen-doped carbon hollow nanospheres support.

LaMnO₃ Perovskite nanoparticles were used by Türkmen and coworkers in 2021 [79] for the promotion of the oxidative C(sp³)-H activation of alkylarenes by using O₂ (1 bar) as the sole oxidant and heptane as the reaction medium at 80 °C. The proposed mechanism involves the formation of surface-bound superoxide anions by the activation of O₂ on the surface of LaMnO₃ and the successive abstraction of the benzylic hydrogen atom producing the radical intermediate. High yields of ketones were obtained, but the used regeneration protocol did not allow the fully recovery of the initial activity of the spent catalyst.

In 2022, Mg₆MnO₈ murdochite nanoparticles were used by Hara and coworkers [80] in the C-H oxidation of a wide variety of alkylarenes to ketones at 50 °C in the presence of O₂ (1 atm) as the sole oxidant and *n*-octane as the reaction medium. On the basis of kinetic and mechanistic studies, it was hypothesized that the oxidation proceeds via a basicity-controlled C-H activation mechanism involving O₂ activation. The murdochite was recovered and reused for 6 runs without changing its high catalytic activity (from 96 to 99% yield).

In the same year, Wang and coworkers [73] designed copper nanoparticles supported on porous amide and ether functionalized organic polymer (Cu@AEPOP) as a heterogeneous catalyst for the efficient oxidative C-H bond activation of alkyl arenes to ketones (93–99% yield). The copper nano-catalyst showed remarkable activity at 70 °C, in the presence of TBHP, 70 wt% in water, which was used as the oxidant and the solvent. Hot filtration experiments showed that no Cu ion was leached into the solution and that heterogeneous catalysis was operative: Cu²⁺ nanoparticles promote the decomposition of TBHP with the formation of surface radical species responsible for C-H benzylic activation by the chain-propagating steps.

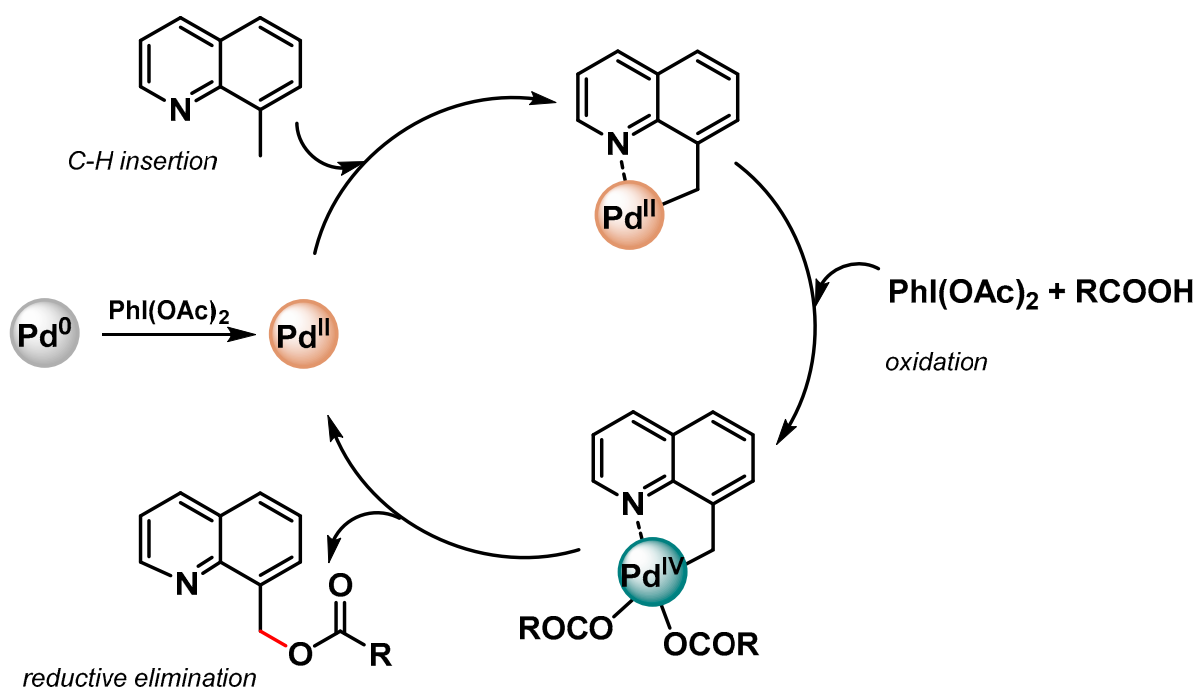
In 2015, Ellis and coworkers [81] reported the preparation of Pd NPs supported on multiwalled carbon nanotubes (Pd(II)/MWCNT) for the oxidative C(sp³)-H activation of 8-methylquinoline in the presence of PhI(OAc)₂ as the oxidant (Scheme 10). When the reaction was performed in MeOH as a solvent, a near-quantitative yield (99%) of 8-(methoxymethyl)quinoline was obtained in 10 min at 100 °C, while in acetic acid at 120 °C for 10 min, the desired 8-(acetoxymethyl)quinoline was obtained in 90% yield. The authors showed that the reactions were faster with Pd(II)/MWCNT than with homogeneous Pd(OAc)₂ (Scheme 10). The catalyst was recycled 16 times with minimal reduction of catalytic activity (from 98 to 90% conversion) and very little metal leaching.



Scheme 10. Oxidative C(sp³)-H activation of 8-methylquinoline.

More recently, Zhang and coworkers [82] prepared monodisperse CuPd alloy nanoparticles supported on reduced graphene oxide (CuPd/rGO) as efficient catalyst for the directed C(sp³)-H activation of 8-methylquinolines in the presence of PhI(OAc)₂ as the oxidant and carboxylic acids to form the corresponding 8-(acyloxymethyl)quinoline.

In both papers [81,82], a N-directing group assisting the Pd(II)/Pd(IV) mechanism via a cyclopalladated intermediate was reported (Scheme 11).

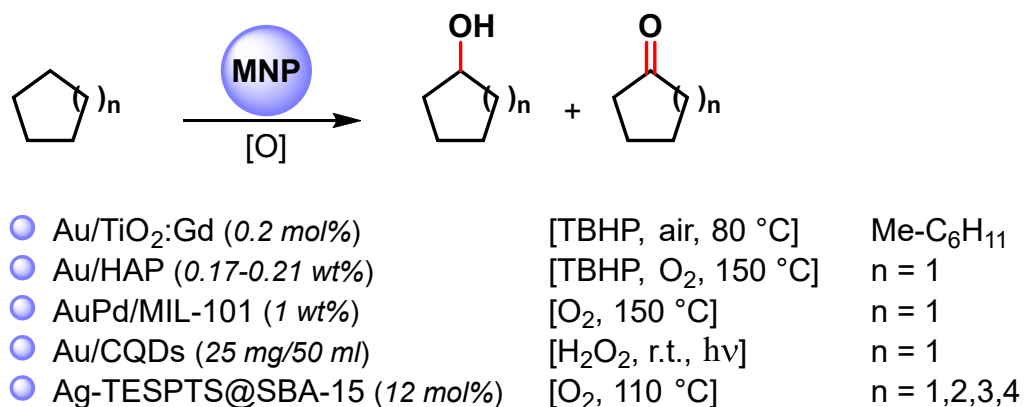


Scheme 11. Proposed mechanism for N-chelation-directed Pd(II)/Pd(IV) C–H activation.

2.3. Cycloalkane C(sp³)–H Activation

The catalytic oxidative C–H activation of cycloalkanes under mild conditions is one of the principal objectives of catalysis chemistry. Indeed, cycloalkanols and cycloalkanones are involved in the production of commodity chemicals, such as polymers, paints, plastics, etc. For example, the oxidative C–H activation of cyclohexane to cyclohexanone and cyclohexanol is the key step of the commercial production of nylon-6 and nylon-6,6 polymers.

Among the metal nanoparticles, Au NPs have been widely used in the oxidative C–H activation of less reactive cycloalkanes (Scheme 12) [67,83–86].



Scheme 12. Oxidative C–H activation of cycloalkanes.

In 2010, Caps and coworkers [83] prepared Au NPs supported on gadolinium-doped titania (Au/TiO₂:Gd) with < 3 nm average size. The catalyst efficiently catalyzed, at 80 °C, in the presence of TBHP and aerobic conditions the methylcyclohexane/stilbene co-oxidation reaction, which led to the formation of 1-methylcyclohexanol. The oxidation proceeds via a complex radical chain mechanism in which Au NPs activate TBHP and produce an alkylperoxy radical through a reaction of a tertiary alkyl radical with atmospheric O₂.

In 2011, Tsukuda and coworkers [84] synthesized ultrasmall Au NPs (<2 nm) with atomically controlled sizes (Au_n, with n = 10, 18, 25, 39) immobilized on hydroxyapatite (Au/HAP) for the selective C–H oxidation of cyclohexane to cyclohexanol and cyclohex-

anone, at 150 °C, in the presence of TBHP and O₂ as oxidants. The turnover frequency increased with an increase in the size, reaching values as high as 18 500 h⁻¹ Au atom⁻¹ at $n = 3$, and thereafter decreased with a further increase in size.

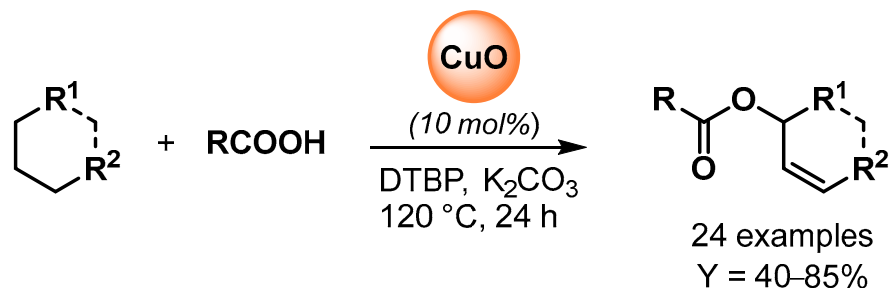
The effect of Au nanoparticle size on catalytic activity was also observed by Golovko and coworkers [87] in the aerobic oxidation of the allylic C–H bond of cyclohexene under mild conditions (65 °C). The authors showed that catalytic activity was observed only when >2 nm Au nanoparticles size had formed, while <2 nm particles were inactive in cyclohexene oxidation. The size dependency observed suggested that Au NPs promote the abstraction of allylic hydrogen with the formation of a cyclohexenyl radical that then reacts with dissolved O₂.

In 2013, bimetallic AuPd NPs supported on zeolite-type metal-organic frameworks (AuPd/MIL-101) were obtained by Li and coworkers [85]. The AuPd alloy catalyst was used in the selective C–H oxidation of cyclohexane at 150 °C in the presence of O₂ as the sole oxidant with high TOF (19 000 h⁻¹) and >80% selectivity to cyclohexanone and cyclohexanol. The Au–Pd bimetallic catalysts showed a higher catalytic activity than pure metal or Au+Pd physical mixture in terms of cyclohexane conversion, suggesting that the enhanced surface electron density of the bimetallic Au–Pd catalyst, compared with monometallic Au, favors O₂ adsorption and activation to form a surface superoxo species.

In 2014, Zhang and coworkers [86] reported the preparation of Au NPs supported on carbon quantum dots (Au/CQDs) and their use in the photocatalytic selective C–H oxidation of cyclohexane to cyclohexanone at room temperature, under visible-light irradiation and in the presence of H₂O₂ as an oxidant. The best conversion efficiency (63.8%) and selectivity (99.9%) was obtained under green-light irradiation, which matches with the surface plasma resonance zone of AuNPs. Light absorption enhanced the catalytic activity of Au/CQDs toward H₂O₂ decomposition to hydroxy radicals, suggesting that HO· is the active oxygen species for this photocatalytic C–H activation.

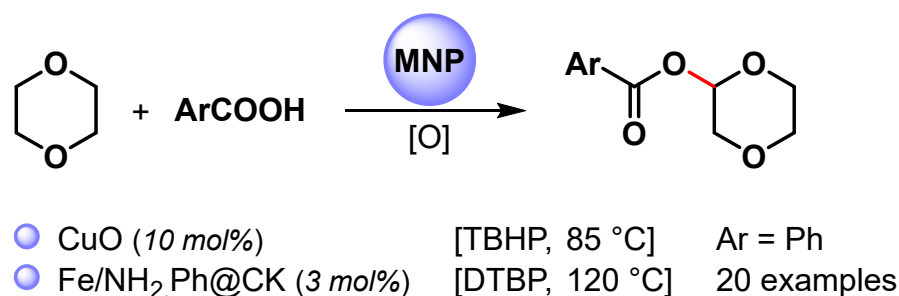
More recently, highly dispersed Ag NPs supported over 2D hexagonally ordered functionalized mesoporous silica material (Ag-TESPTS@SBA-15, AgMS) was reported by Biswas and coworkers [67]. Alongside the selective benzylic C(sp³)–H bond oxidation of toluenes and alkyl arenes to the corresponding carbonyl compounds described above, the authors showed that the catalyst was also active in the oxidative C–H activation of less reactive cyclic alkanes to ketones with good yield (61–69%) and selectivity (73–81%).

The copper-catalyzed oxidative esterification of carboxylic acids with common alkanes via C(sp³)–H bond dehydrogenation was reported by Li and coworker in 2015 [62]. The preparation of allylic esters was catalyzed by CuO in the presence of di-*tert*-butylperoxide (DTBP) as oxidant and a catalytic amount of K₂CO₃ as promoter (Scheme 13). Radical inhibitors, such as TEMPO, completely suppressed the reaction, indicating a radical pathway for the C–H oxidative dehydrogenation and esterification cascade.



Scheme 13. Copper-catalyzed oxidative coupling of carboxylic acids with alkanes.

The direct esterification of benzoic acid with cyclic ether via C(sp³)–H bond activation by using non-noble metal nanoparticles was firstly reported by Kantam and coworkers in 2015 [88] and then by Jia and coworkers in 2021 [89] (Scheme 14) [88,89].



Scheme 14. Direct esterification of benzoic acids with cyclic ether via C(sp³)-H bond activation.

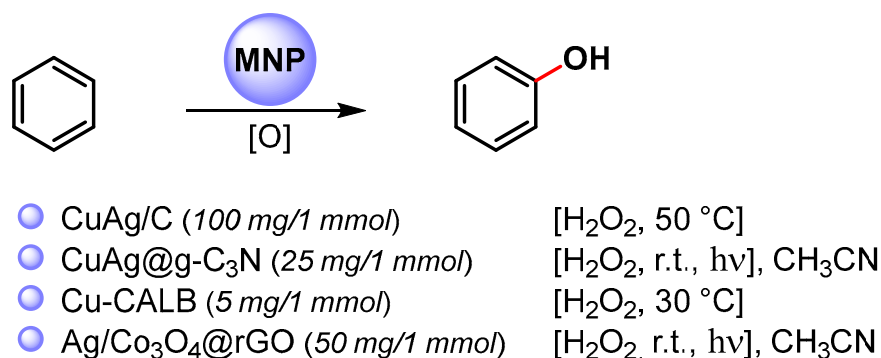
When CuO nanoparticles were used in the presence of TBHP as an oxidant at 85 °C, 1,4-dioxane underwent a cross-dehydrogenative coupling reaction with benzoic acid, producing the corresponding benzoate in 91% yield [88].

A wide variety of α -acyloxy ethers were obtained in moderate to good yields (up to 75%) via the direct cross-dehydrogenative-coupling reaction of arylcarboxylic acids with cyclic ethers by using Fe NPs supported on organo-modified coal-bearing kaolin (NH₂,Ph@CK) as a heterogeneous catalyst and DTBP as an oxidant at 120 °C [89]. The competing kinetic isotope effect (1,4-dioxane/1,4-dioxane-d₈, $k_H/k_D = 2.5$) and control experiments with TEMPO suggested a radical pathway in which the C(sp³)-H bond cleavage of ether was the rate-determining step.

2.4. Aromatic C(sp²)-H Activation

The direct C(sp²)-H activation of aromatics by using metal and metal-oxide nanoparticles has been widely explored, but the preparation and the use of cost-effective nanocatalysts under milder reaction conditions remain a challenge.

In particular, the synthesis of phenols is a very important process in the fine-chemical industry and their preparation by direct C-H hydroxylation is highly desirable. Recent examples of the direct C-H functionalization of benzene to phenol, catalyzed by metal nanoparticles, are shown in Scheme 15 [76,90–92].



Scheme 15. Direct hydroxylation of benzene via C-H activation.

In 2016, Jiang and coworkers [90] reported the preparation of bimetallic Cu-Ag NPs supported on biochar (Cu-Ag/C) obtained by the one-pot fast pyrolysis of Cu-Ag preloaded onto biomass waste and its use in the direct hydroxylation of benzene to phenol by using H₂O₂ as an oxidant at 50 °C. The best reaction yield (35%) and selectivity (96%) was obtained with acetic acid as the reaction medium. The catalyst showed only a slightly decrease of performance over three consecutive runs, indicating that Cu-Ag/C has good reusability.

A year later, Varma and coworkers [91] used photoactive bimetallic Cu-Ag NPs immobilized onto a graphitic carbon nitride surface (CuAg@g-C₃N) for the C-H activation and hydroxylation of benzene. Quantitative conversion was obtained in 30 min, in CH₃CN, by using H₂O₂ as an oxidant, at room temperature under visible-light irradiation (20 W domestic bulb). In dark conditions, the reaction did not proceed. Graphitic carbon nitride

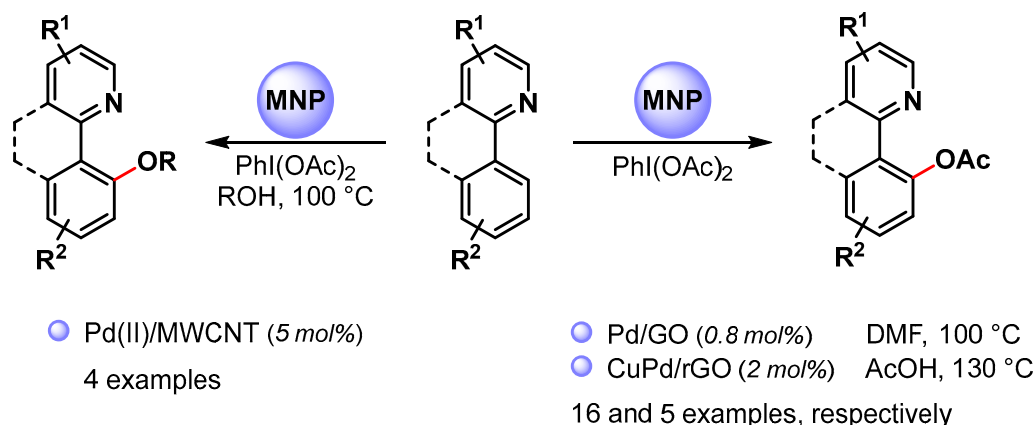
support absorbs the visible light promoting the degradation of hydrogen peroxide into hydroxyl radicals.

In both papers [90,91], it was shown that bimetallic Cu-Ag NPs were more active than monometallic Cu or Ag NPs, suggesting a synergistic effect between Ag and Cu in the formation of the hydroperoxide radical and the activation of the C–H bond on the benzene ring. Moreover, it was hypothesized that the carbonaceous supports grip benzene molecules on its surface through non-covalent interactions, thus facilitating the C–H bond breaking and the attack of HO·.

In 2020, Palomo and coworkers [92] synthesized nanobiohybrids containing copper nanoparticles by using the enzyme Lipase B from *Candida antarctica* (CAL-B) in combination with copper sulfate. Depending on the experimental conditions, enzymes facilitate the formation of a particular Cu species, such as Cu(0)NPs, Cu(0)/Cu₂ONPs, Cu₂ONPs or Cu₃(PO₄)₂NPs. The catalytic activity of heterogeneous enzyme–copper nanobiohybrids was evaluated with the direct C–H activation hydroxylation of benzene using H₂O₂ as an oxidant, in aqueous medium at 30 °C. The enzyme-copper nanobiohybrid obtained in phosphate buffer without treatment with a reducing agent (Cu-CALB-PHOS-NR) showed the highest activity, and, when the hydroxylation was carried out in the presence of 20% acetonitrile as co-solvent, phenol was obtained with 24% yield and 83% selectivity. A radical mechanism that involves the degradation of H₂O₂ via a Fenton-like reaction to produce a hydroxyl radical and Cu(III) was hypothesized.

In same year, Zhang and Liu [76] reported the preparation of small-sized Ag NPs (2–10 nm) supported on Co₃O₄ nanoparticles embedded on the surface of reduced graphene oxide. The photocatalyst efficiently catalyzed the hydroxylation of benzene to phenol via C–H activation in acetonitrile, under visible-light irradiation. A conversion of 99% and 96% phenol selectivity was obtained in 30 min. The high catalytic activity was ascribable both to the high dispersion of the nanocomposite over the support and to the high surface area. The nanocomposite was conveniently recovered and reused for seven runs without the loss of its catalytic activity (≥98% conversion, ≥95% selectivity). The formation of phenol takes place via a radical pathway on the surface of the photocatalyst where the photo-active bimetallic NPs promote the degradation of hydrogen peroxide into hydroxyl radical and the noncovalent interactions of benzene with graphene surface activate the substrate toward C–H hydroxylation.

High selective C–O bond formation via the C(sp²)–H bond activation of aromatic compounds can be achieved by using palladium catalysis combined with an intramolecular directing group, such as a pyridinyl or other nitrogen-functional groups. In most cases, homogeneous Pd(II) catalysts are used, and only a few examples have been reported in the use of heterogeneous Pd NPs (Scheme 16) [81,93,94]. Generally, these reactions utilize a Pd(II)/Pd(IV) catalytic cycle (see Scheme 11) [81,82].



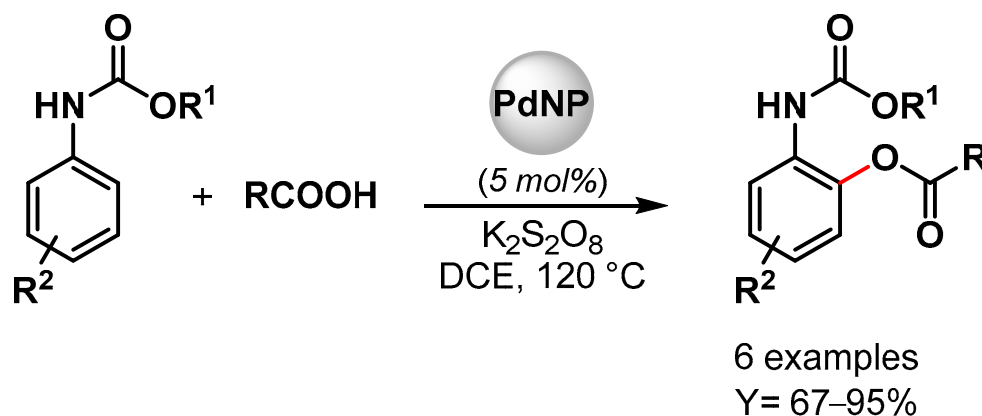
Scheme 16. N-Chelation-directed C(sp²)–H activation for C–O bond formation.

In 2015, Ellis and coworkers [81] used Pd(II) NPs supported on multiwalled carbon nanotubes (Pd(II)/MWCNT) in the selective N-chelation-directed C–H activation reactions of benzo[h]quinoline in the presence of $\text{PhI}(\text{OAc})_2$ as an oxidant and alcohols as a solvent at 100 °C. When methanol was used as a solvent, 9-methoxy-derivatives were obtained in high yield (90%). However, as the size of the alcohol increased (ethanol, isopropanol), the product yield decreased (73% and 33%, respectively), and, in the case of *tert*-butyl alcohol, no product was observed.

In 2017, Junmin Zhang and coworker [93] reported the use of Pd NPs supported on graphene oxide (Pd/GO) for the selective acetoxylation of 2-aryl pyridines by using $\text{PhI}(\text{OAc})_2$ as an oxidant in DMF at 100 °C. High yields were obtained for a wide variety of substrates (up to 98%), and the authors showed that the catalytic efficiency of PdNPs/GO was superior to that of free $\text{Pd}(\text{OAc})_2$. A hot filtration test and a Hg poisoning test suggested a heterogeneous catalysis but a recycling test showed a drastic decrease in yield on the third run. This was mainly attributed to palladium leaching in the reaction medium (>40% in the first cycle) and to Pd NPs aggregation.

More recently, Wu Zhang and coworkers [94] prepared CuPd alloy nanoparticles immobilized on reduced graphene oxide (CuPd@rGO) for the N-chelation assisted C(sp²)–H bond acetoxylation using different directing group, including pyridine, pyrazole, benzothiazole and pyrimidine. The reactions were performed in chlorobenzene in the presence of $\text{PhI}(\text{OAc})_2$ and acetic acid at 130 °C. Acetoxy derivatives were obtained in moderate to good yield, and the best result was obtained with pyridine as the directing group (90% yield). The catalyst was recovered and reused for five cycles with only a slight decrease in catalytic activity (from 94 to 85% yield).

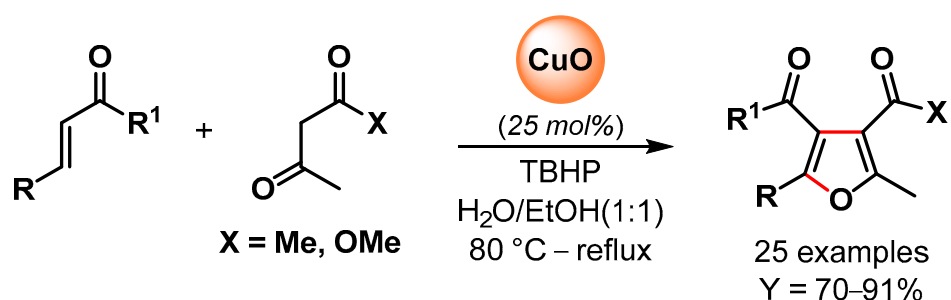
In 2022, high-performance Pd NPs supported on nitrogen-doped reduced graphene oxide (Pd/N-RGO) were developed by Movahed and coworker [95]. The nanohybrid catalyst was used as a heterogeneous catalyst for the *ortho* C–H acyloxylation of *N*-arylcarbamates with carboxylic acid in the presence of $\text{K}_2\text{S}_2\text{O}_8$ as an oxidant in dichloroethane (DCE) at 120 °C (Scheme 17). Good yields were obtained with both aliphatic and aromatic carboxylic acid (up to 95%), but bulky alkyl side-chain carboxylic acid (*t*-Bu and *i*-Pr) showed no reactivity. Moreover, the presence of an electron-donating group on phenyl-carbamate led to a higher yield compared to the electron-withdrawing group. These effects, together with the experiment on the radical scavenger TEMPO that showed no effect on the reaction yield, were consistent with an electrophilic palladation pathway with the formation of a cyclopalladated intermediate in which $\text{K}_2\text{S}_2\text{O}_8$ plays an important role in maintaining the Pd(II)/Pd(0) and Pd(II) Pd(IV) catalytic cycle. The heterogeneous catalyst was reused ten times (from 93 to 75% yield), and additionally, when the $\text{Pd}(\text{OAc})_2$ homogeneous catalyst was used, only a moderate yield was obtained, indicating that the nitrogen-doped graphene support could improve the activity and the stability of the Pd catalyst.



Scheme 17. Pd/N-RGO-catalyzed C–H acyloxylation of *N*-arylcarbamates.

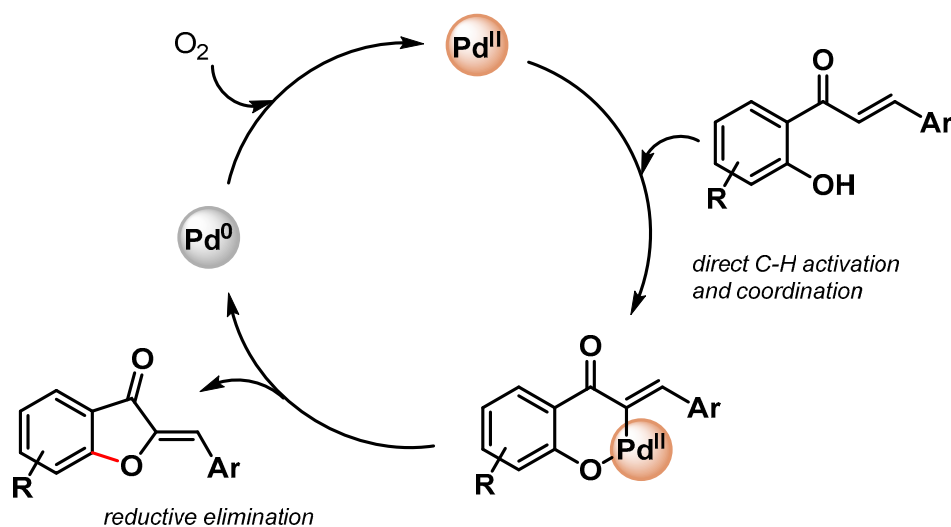
2.5. Olefinic C(sp²)-H Activation

In 2016, Banerjee and coworkers [96] reported the synthesis of poly-substituted furans via the oxidative C-H/C-H functionalization of 1,3-dicarbonyls and α,β -unsaturated carbonyl compounds catalyzed by CuO nanoparticles in the presence of TBHP as an oxidant in aqueous ethanol as a green solvent (Scheme 18). A control experiment with TEMPO suppressed the reaction, indicating a radical pathway with CuO nanoparticles promoting the decomposition of TBHP with the formation of surface radical species that activated the C(α)-H abstraction of 1,3-dicarbonyl and the successive conjugate addition/domino reactions. High yields of substituted furans were obtained for a large number of substrates, and good recyclability was obtained for up to six cycles, but a slight drop in the yield was observed thereafter (from 81 to 70% yield). The XRD pattern of recycled CuO NPs after the fourth run showed that the morphology of the particles was unchanged but that the size increased from 10 to 15 nm.



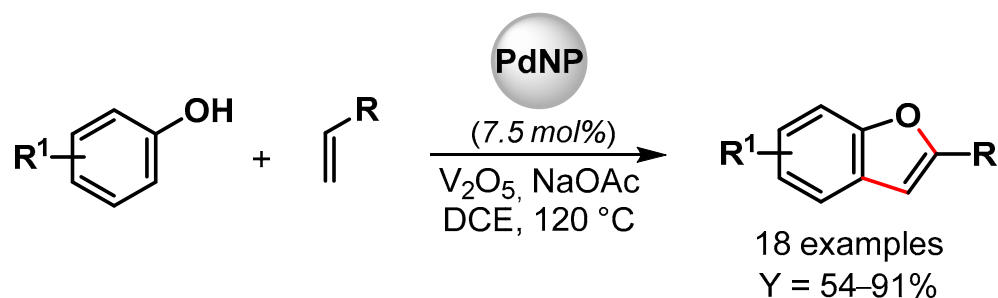
Scheme 18. CuO NPs catalyzed synthesis of substituted furans via oxidative C-H/C-H functionalization in aqueous medium.

In 2018, Yamaguchi and coworkers [97] reported the preparation of aurones, unusual five-membered ring flavonoids, via the direct α -olefinic C-H activation of chalcones by using Pd-on-Au bimetallic NPs supported by a CeO₂ catalyst (Pd/Au@CeO₂, 5 mol%) under air at 100 °C (Scheme 19). Moderate to good yields (16–72%) with high Z-selectivity (93–99%) in the aurone products were obtained. The monometallic Pd@CeO₂ showed very low conversion, while Au@CeO₂ was highly active, but the formation of a six-membered flavone was observed. The authors hypothesized that the role of Au was to stabilize and improve the catalytic activity of Pd(0) NPs. The control experiment showed that the reaction rate was not affected by adding the radical scavenger TEMPO, suggesting Pd(0)/Pd(II) α -olefinic C-H bond activation with the formation of a six-membered palladacycle intermediate.



Scheme 19. Preparation of aurones via direct Pd/Au@CeO₂ catalyzed α -olefinic C-H activation of chalcones.

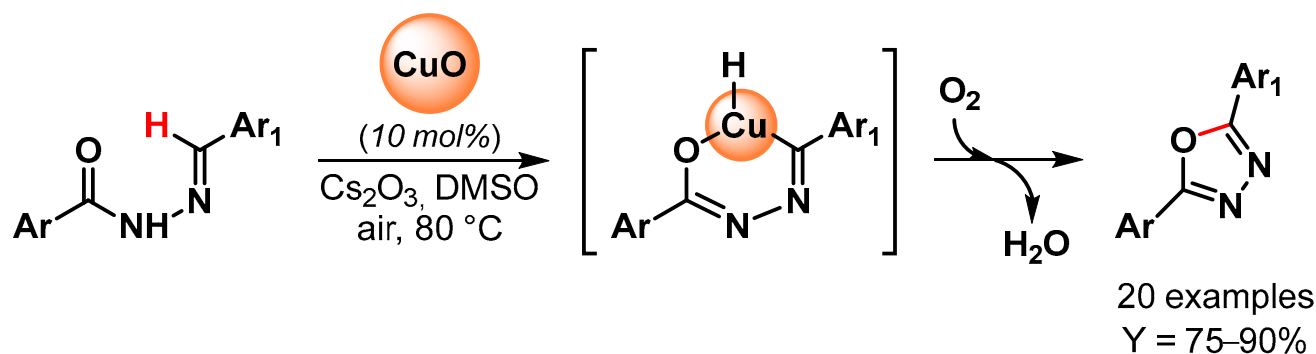
In 2019, Maji and coworkers [98] prepared Pd nanoparticles deposited on amyloid fibril (α -Syn-PdNPs), a sustainable catalyst for the preparation of benzofuran involving C–C and C–O bond formation via the triple C–H bond activation of phenols and alkenes (Scheme 20). Among various oxidants, the best results were obtained with V_2O_5 , and good to excellent yields (up to 91%) were obtained for a wide variety of substrates. The heterogeneous Pd nanocomposite was reused for up to four runs with a negligible loss of catalytic activity (from 95 to 90% yield). A plausible mechanism for the formation of benzofuran via the insertion of Pd(0) at the ortho position of phenol and the successive coordination and migratory insertion of the olefin at the Pd(II) center was hypothesized.



Scheme 20. Preparation of benzofuran via C–H activation using amyloid fibril-supported PdNPs.

2.6. Formyl C(sp²)–H Activation

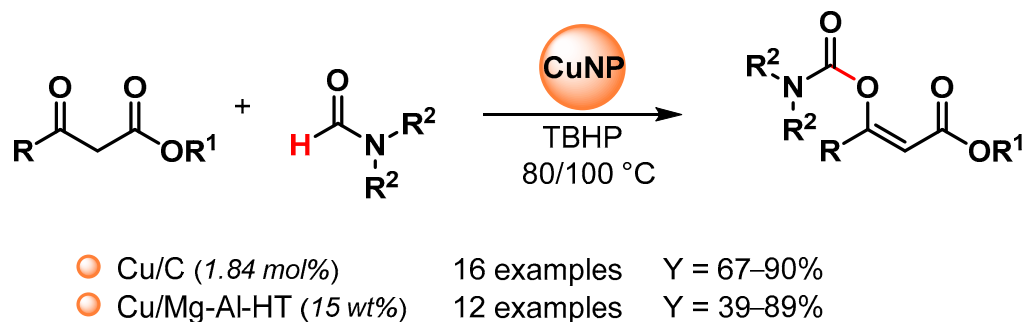
In 2014, 2,5-disubstituted 1,3,4-oxadiazoles have been synthesized by Bojja and coworkers [99] through oxidative C–O coupling via the direct C–H bond activation of *N*-aroyl-*N*-arylidinehydrazines using CuO nanoparticles as a catalyst (Scheme 21). Performing the reactions in the presence of Cs_2CO_3 as a base, in DMSO, under air at 80 °C, excellent to good yields were obtained for a large number of substrates. Moreover, an electron-withdrawing substituent on the arylidenehydrazine moiety improved the yields, probably through an increment of the acidity of the imine proton and thus facilitating the metalation step. The catalyst has been reused for three times with a negligible decrease in catalytic activity (from 90 to 85% yield).



Scheme 21. Synthesis of 2,5-disubstituted 1,3,4-oxadiazoles via direct oxidative C–H bond activation.

Recently, copper nanoparticles were investigated as environmentally friendly heterogeneous catalysts for the synthesis of enol carbamates via the oxidative coupling of *N,N*-dialkyl formamides with β -ketoesters [100,101] (Scheme 22).

In 2016, Niknam and coworkers [100] reported the use of copper NPs on charcoal (Cu/C) as an effective nano-catalyst for enol carbamates synthesis via the C–H bond activation of dialkylformamides by using TBHP as an oxidant at 80 °C (Scheme 22). The catalyst was reused at least five times with no appreciable loss in catalytic activity (from 85 to 75% yield).



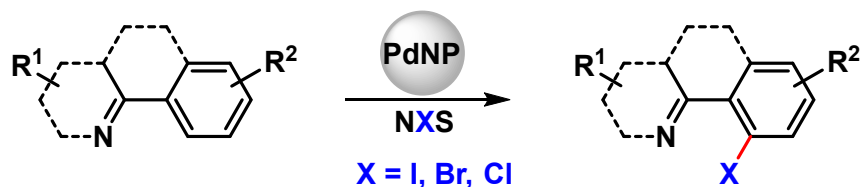
Scheme 22. Copper catalyzed enol carbamates synthesis via direct C–H activation of dialkylformamide.

In 2020, Mannepalli and coworkers [101] described the preparation of a copper-supported Mg-Al hydrotalcite-derived oxide catalyst (Cu/Mg-Al-HT) by a co-precipitation method, followed by wet impregnation and calcination and its use in enol carbamates synthesis via the oxidative C–H bond activation of dimethylformamide by using TBHP as an oxidant at 100 °C (Scheme 22). The catalyst was recovered and reused for up to four runs without a loss in catalytic activity (from 89 to 87% conversion). Mechanistically, β -ketoester forms a coordination complex with copper, and the complex decomposes TBHP to generate the *tert*-butyloxy radical that can abstract the formamide hydrogen on the copper surface.

3. Carbon–Halogen (C–X) Bond Formation

Halogenated compounds are useful intermediates in industrial productions, as they can be further transformed to synthesize widely diverse structures.

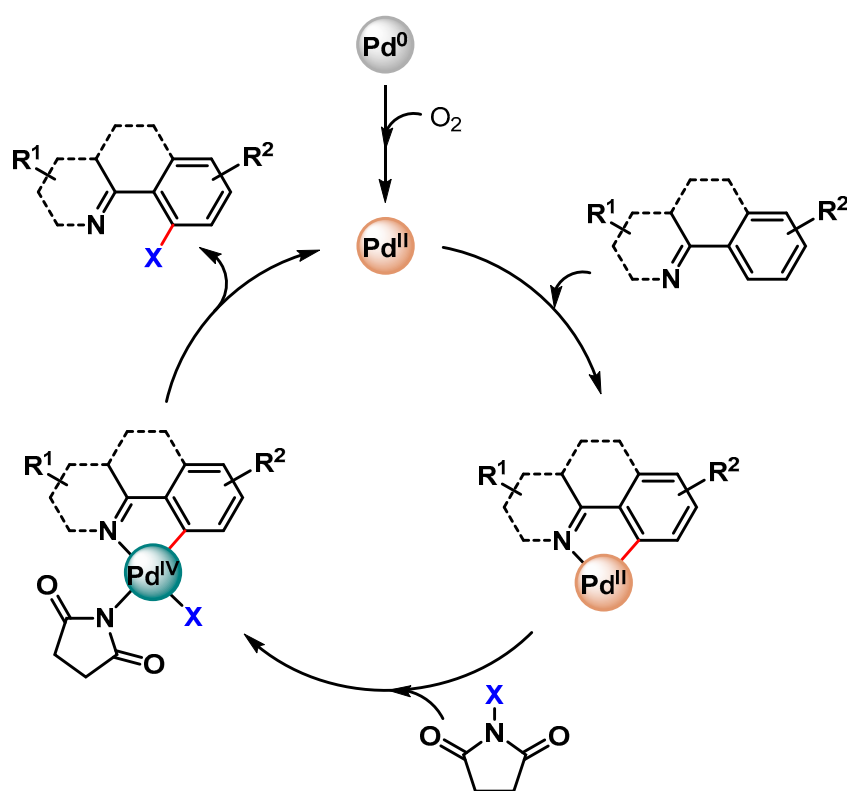
Selective C–H functionalization can be an effective tool for their preparation and can be highly desirable, but the formation of a C–halogen bond by oxidative C–H activation has been rarely performed using metal nanoparticles as catalysts. Pd NPs have been used to this end for *N*-chelation assisted C(sp²)–H activation (Scheme 23) [81,93,95,102,103].



- Pd(II)/MWCNT (5 mol%) CH₃CN or AcOH, 100–120 °C 8 examples
- Pd NPs (3 mol%) C₆H₆, PhICl₂, 120 °C 2 examples
- Pd@MOF (4 mol%) AcOH, air, 50 °C 12 examples
- Pd/GO (0.8 mol%) DMF, 100 °C 3 examples
- Pd/N-RGO (5 mol%) DCE, 100 °C 6 examples

Scheme 23. Pd NPs catalyzed *N*-chelation assisted C(sp²)–H activation for C–X bond formation.

The proposed mechanism involves an initial oxidation of Pd(0) to Pd(II), which, by *N*-directing group assistance, is then involved in the Pd(II)/Pd(IV) catalytic cycle via the cyclopalladated intermediate (Scheme 24).



Scheme 24. Possible reaction mechanisms for Pd-catalyzed C–H halogenation.

Pd(II) NPs supported on multiwalled carbon nanotubes (Pd(II)/MWCNT) prepared by Ellis and coworkers in 2015 [81], also effective for C–O bond formation, were also used in C–Cl and C–Br formation via selective *N*-chelation-directed C(sp²)–H activation in the presence of *N*-chloro- (NCS) or *N*-bromo-succinimide (NBS), using acetonitrile or acetic acid as a solvent at 100 and 120 °C, respectively. High to moderate yields (30–92%) were obtained, and, as noted for C–O bond formation, halogenation reactions were faster with Pd(II)/MWCNT than with homogeneous Pd(OAc)₂.

In 2017, Kim and coworkers [102] reported the preparation of small sized Pd NPs (3.5 nm) by the thermal decomposition of [Pd(acac)₂] in the presence of oleylamine and trioctylphosphine. By the controlled oxidation of Pd(0)NPs with PhICl₂ in benzene at 120 °C, the more active Pd(IV) surface clusters were formed and characterized by XPS. After the completion of a halogenation reaction performed in the presence of NCS or NBS (99% yield), Pd(0) species were regenerated, opening the route for a tandem reaction that combined C–H halogenation, catalyzed by Pd(IV) species, with a cross-coupling reaction, catalyzed by Pd(0), for the formation of new C–C, C–N and C–S bonds.

In 2016, very small-sized Pd NPs (2 nm), immobilized onto porous Fe-based or Cr-based MOFs (Pd@MOFs), were developed by Martín-Matute and coworkers [103]. The catalysts were used for *N*-chelation-directed aromatic C–H activation/halogenation. *N*-iodo, *N*-bromo or *N*-chlorosuccinimide were used as the corresponding halogen sources under very mild reaction conditions and in short reaction times. Very high conversions (up to 99%) were achieved with both catalytic systems for a wide range of aromatic compounds containing pyridine or amides as directing groups. Selectivity between mono- and di-halogenated products could be fully controlled by finely tuning the reaction conditions. Moreover, these catalysts showed extremely low metal leaching and very good recyclability (>99% conversion for five runs). A rapid leaching–deposition mechanism was proposed by the authors.

In 2017, Zhang and coworker [93] prepared Pd NPs immobilized on graphene oxide (Pd/GO). Besides the abovementioned selective acetoxylation of 2-aryl pyridines, the authors showed that the catalyst was also active in the direct C–H halogenation of

2-phenylpyridine in the presence of *N*-halogenosuccinimide in DMF at 100 °C. A high yield was obtained only for the bromination reaction (81%), while low yield (15%) and no desired product could be obtained for chlorination and iodination, respectively.

Pd NPs supported on nitrogen-doped reduced graphene oxide (Pd/N-RGO) developed by Movahed and coworker in 2022 [95], above described as a heterogeneous catalyst for the *ortho* C–H acyloxylation of *N*-arylcarbamates, were also used in the *N*-directed C–H halogenation of 2-arylquinazolinones with NBS or NCS in DCE at 100 °C. The presence of *p*-toluenesulfonic acid as the acidic additive was critical to obtain high performance, and, as reported for acyloxylation, higher yields were obtained for substrates containing electron-donating groups than for electron-withdrawing groups, thus indicating the in situ formation of the electron-deficient Pd complex.

In 2017, Ackermann and coworkers [104] paved the route to the *meta*-C–H bromination of purine bases via remote C–H activation catalyzed by a heterogeneous ruthenium catalyst (Ru@SiO₂). The reactions were performed under air in the presence of NBS, with *N,N*-dimethylacetamide as a solvent at 80–100 °C (Scheme 25). The Ru@SiO₂ catalyst outperformed the homogeneous RuCl₃ catalyst and promoted the *meta*-C–H halogenation of a wide variety of substrates with excellent positional selectivity and unique catalytic efficacy. Moreover, the authors showed that solely ruthenium catalysis regime provided access to meta halogenate purine derivatives, illustrating the unique synthetic utility of ruthenium-catalyzed C–H activation. The heterogeneous catalyst was easily recovered and reused for up to seven runs: excellent recyclability was obtained for five cycles, but a slight drop of yield was observed thereafter (from 62 to 43% yield). XPS and SEM studies on the recovered catalyst revealed a shift in the nature and oxidation state of the ruthenium active sites.

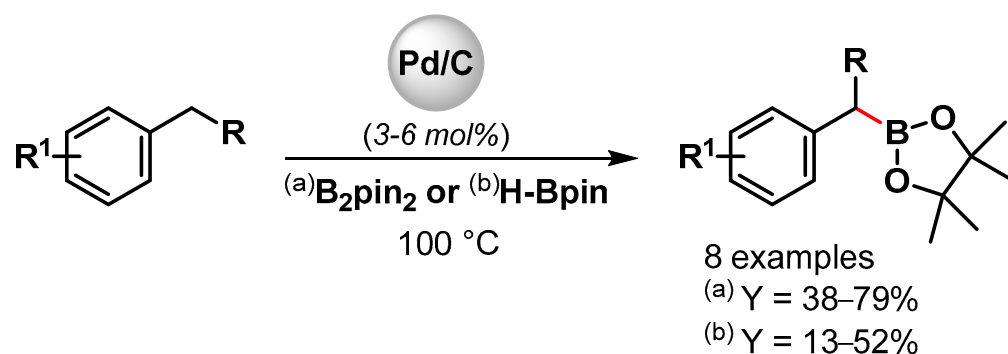


Scheme 25. Ru@SiO₂ catalyzed remote *meta*-C–H bromination of aryl purines and heteroarenes.

4. Carbon–Boron (C–B) Bond Formation

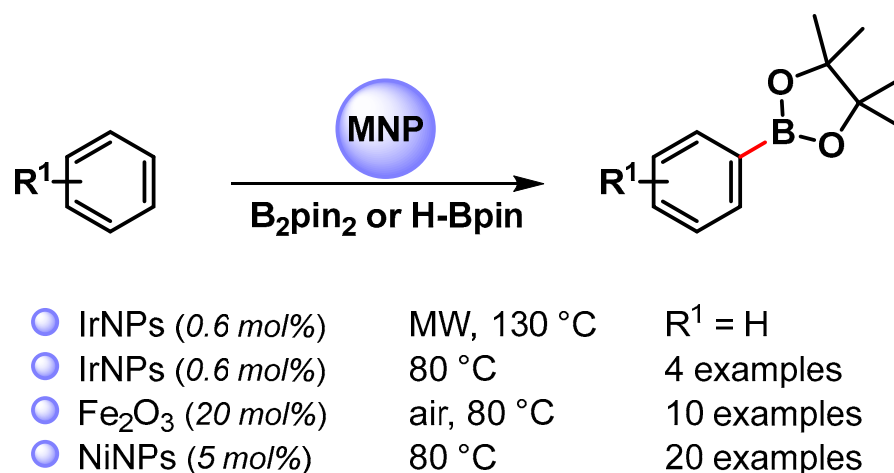
Organoboron compounds are considered extremely useful reagents since they are versatile intermediates in organic synthesis and pharmaceutical chemistry. One of the most effective methods for their preparation is the direct functionalization of C–H bonds using a borane reagent [105]. Apart from transition-metal complexes, only a few examples implying the use of metal nanoparticles have been reported for the catalyzed C–H borylation.

Indeed; a rare example of the direct C(sp³)-H activation/borylation of alkyl benzenes using metal nanoparticles was reported in 2001 by Miyaura and coworkers [106]. Borylation at the benzylic C–H bond with diboron pinacol ester (B₂pin₂) or pinacolborane (H-Bpin) was carried out at 100 °C in the presence of a catalytic amount of Pd/C (Scheme 26). Good yields were obtained by using a diboron pinacol ester, while moderate yields were observed with H-Bpin. A kinetic experiment on the C–H borylation of toluene with B₂pin₂ indicated a two-step process involving a very fast and quantitative reaction of toluene with the diboron pinacol ester, followed by a slow reaction with pinacolborane generated by the former process.



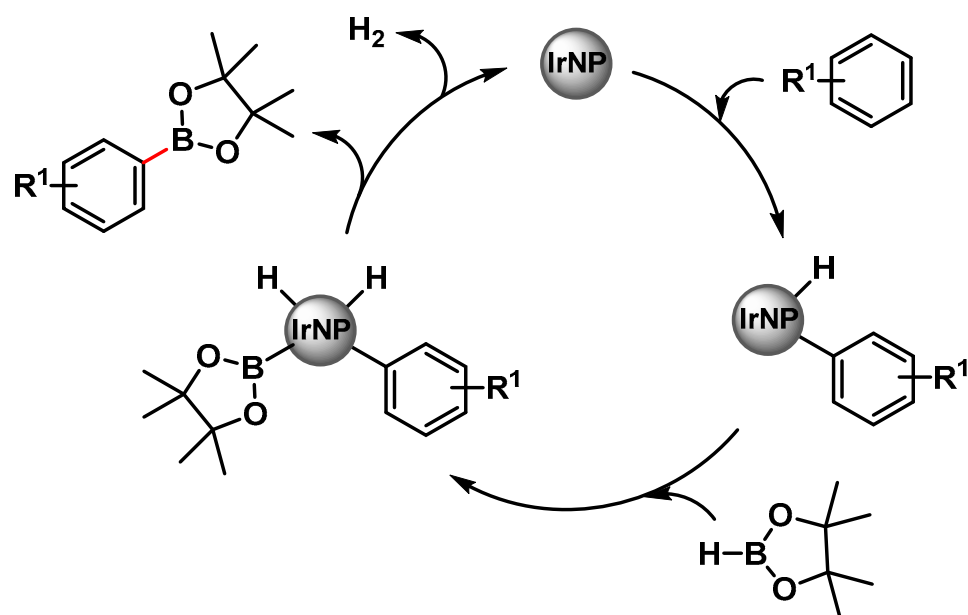
Scheme 26. Pd/C catalyzed the benzylic C–H borylation of alkylbenzene.

The use of metal NPs for the C–B bond formation via the direct C(sp²)–H activation of aromatics has also been rarely investigated (Scheme 27) [107–109].



Scheme 27. Direct C(sp²)–H borylation of aromatics catalyzed by metal nanoparticles.

In 2008, Yinghuai and coworkers [107] reported the preparation of small-sized iridium(0) nanoparticles (3.5 nm) by the reduction of the precursor hydrido-iridium carborene stabilized with the ionic liquid trihexyltetradecylphosphonium methylsulfonate, [THTdP][MS]. The nano-Ir(0) catalyst was found to be highly active in the C–H phenyl-borylation reaction with H-Bpin, under microwave irradiation (130 °C for 1 h), in the presence of tetra-2-pyridinylpyrazine as the base. When the reaction was performed under conventional heating at 80 °C for 20 h, the yield dropped to 47%. Electron-donating groups (R¹ = Me, OMe) decrease the reactivity (39% and 40% yield, respectively) while the electron-withdrawing CF₃ groups led to 89% yield after 12 h. The regioselectivity was not affected from the electronic properties of substituents. Although the definitive mechanism was not clear, it was observed that, when benzene or benzene-d₆ were used as substrates, under the same conditions, a relevant isotope effect was observed (91% vs. 14.3% yield, respectively). This results suggested that iridium(0) was able to activate the C–H bond of the benzene to form the actual active species [Ph–Ir], [Ir–H]. H-Bpin then proceeded to an oxidative addition process leading to iridium species featuring both reactants. The reductive elimination then led to a release of the borylated product and H₂ with the completion of the catalytic cycle (Scheme 28). The catalytic system was recovered and reused at least six times with the negligible loss of its activity (<0.5%).



Scheme 28. Proposed mechanism for the direct C(sp²)-H borylation of aromatics catalyzed by iridium nanoparticles.

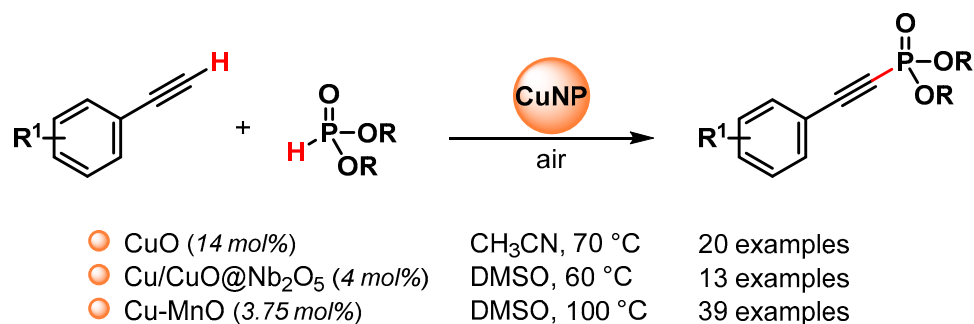
In 2010, Wang and coworkers [108] used a nano-Fe₂O₃ catalyst for the C(sp²)-H bond borylation of arene with B₂pin₂. The best results were obtained in the presence of *tert*-butylperoxide as an oxidant, under open air at 80 °C in the presence of K₂CO₃ as a base. Moderate yield and selectivity, controlled by electronic effects of substituents, were obtained. The mechanism of this aromatic borylation reaction was not clear; indeed the kinetic isotope effect measured was 1.3, and an electrophilic metalation by Fe-B species, followed by reductive elimination, was hypothesized.

In 2019, the nickel-catalyzed C(sp²)-H borylation of arenes was reported by Mandal and coworkers [109]. The reactions were performed in the presence of a well-defined abnormal *N*-heterocyclic carbene-Ni(II) complex that, under the reaction conditions (solvent free at 80 °C), formed Ni nanoparticles (Ni-NPs), able to act as catalytically active species. TEM images showed highly monodisperse nickel nanoparticles with an average size of 3.4 nm, and X-ray photoelectron spectroscopy confirmed the formation of nickel(0). A kinetic isotope experiment with benzene and benzene-d₆ ($K_H/K_D = 1.76$) showed that the breaking of a C(sp²)-H bond was involved in the rate-determining step. The proposed mechanism follows the previously reported iridium nanoparticles catalyzed borylation of arene (Scheme 28) with the activation of either an arene C-H and H-Bpin bond on the surface of Ni NPs and reductive elimination, which leads to the formation of a borylated product with the liberation of H₂, regenerating the active catalyst.

5. Carbon-Phosphorous (C-P) Bond Formation

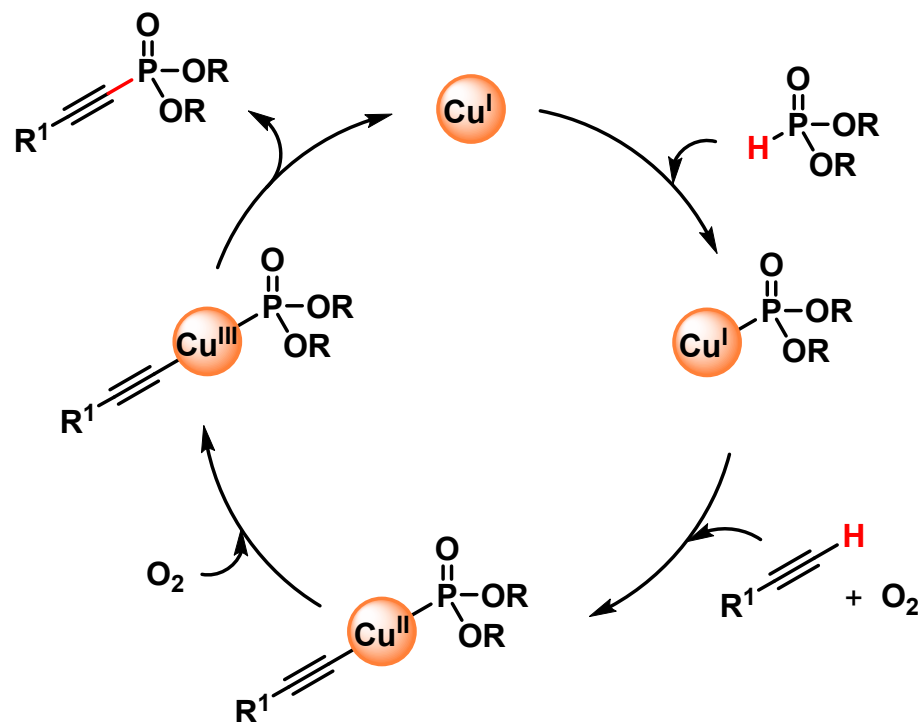
Alkynyl phosphonates, containing reactive triple bonds and phosphoryl groups, are an important class of intermediates that can be transformed into a variety of organophosphorus derivatives, often of interest as biological or pharmacological active compounds [110].

The C(sp)-P bond formation via the direct functionalization of the C(sp)-H bond of the terminal alkyne with H-phosphonates represents the most efficient and atom-economical method for preparing alkynylphosphoryl compounds, and to this end, various copper nano-catalysts have been used to promote this transformation (Scheme 29) [111–113].



Scheme 29. Direct C(sp)-P bond formation from alkynes and phosphite esters catalyzed by Cu nanoparticles under air atmosphere.

In 2016, Radivoy and coworkers [111] reported a mild, base and ligand-free protocol for the direct preparation of alkynyl phosphonates via the C(sp)-H activation of alkynes and H-phosphonates, catalyzed by CuO in acetonitrile at 70 °C under air atmosphere as the sole oxidant. The protocol was compatible with a wide variety of functional groups, and a large number of alkynyl phosphonates were obtained in good to excellent yields (64–97%). The authors observed that the yield was not affected by the addition of TEMPO as a radical scavenger and that the efficiency of the reaction decreased in the absence of oxygen. Furthermore, the results observed by using different solvents were related to the ability of acetonitrile to act as a ligand for copper and speculate that a Cu(I)/Cu(III) catalytic cycle, in which Cu(I)MeCN species react with dialkyl phosphite and the terminal alkyne, was operative (Scheme 30).



Scheme 30. Proposed mechanism for direct C(sp)-P bond formation.

In 2018, Lu and coworkers [112] reported an aerobic oxidative coupling of alkynes and phosphite esters catalyzed by Cu/Cu₂O nanoparticles supported on Nb₂O₅ (Cu/Cu₂O@Nb₂O₅) in the presence of (*n*-Bu)₃N as the base, in DMSO at 60 °C, under air atmosphere. Good to excellent yields (75–93%) were obtained for a wide variety of functional groups in the starting alkynes. Control experiments and characterization data showed that Nb₂O₅ support plays a crucial role in the promotion of the reaction. Indeed, due to its strong Lewis acid sites, it can reduce the electronic density of Cu, favoring the formation of Cu(I) and

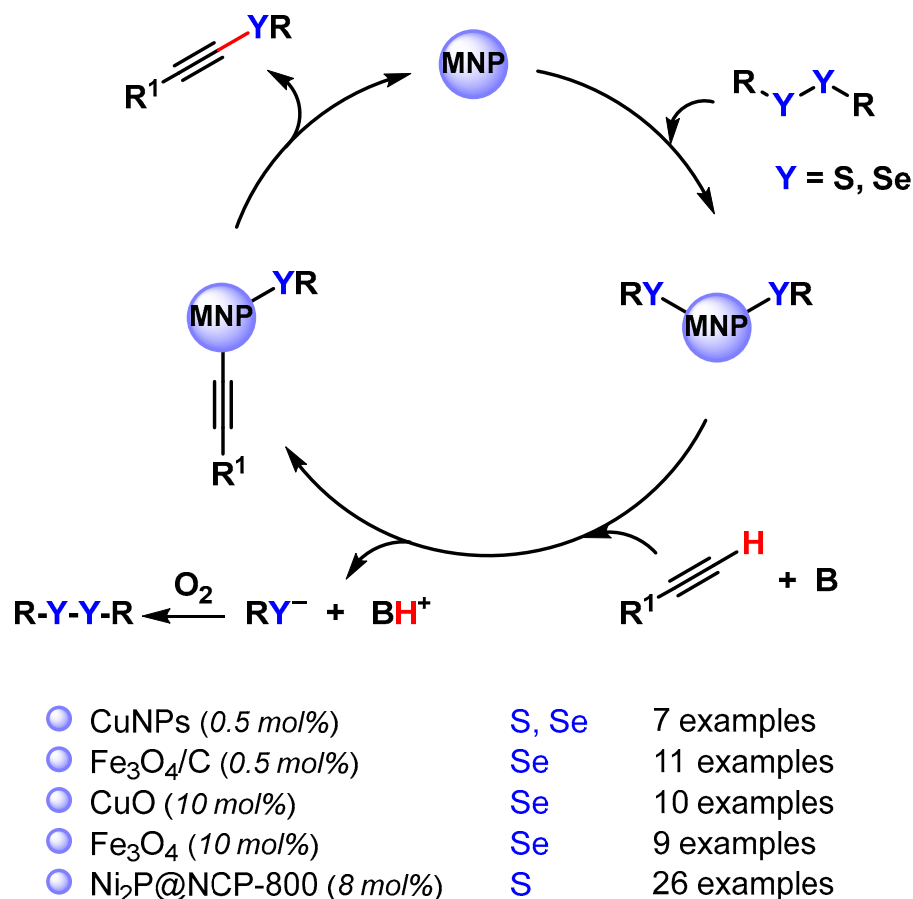
Cu(II) species, and can absorb the phosphite esters favoring the interaction between the catalyst and substrates. The heterogeneous nature of the Cu/Cu₂O@Nb₂O₅ catalyst was demonstrated by a hot filtration experiment and a recycling test showed good recyclability for four runs, while Cu/CuO NPs agglomeration and a drop of the yield were observed in the fifth run.

In 2019, Ghosh and coworker [113] synthesized a recyclable heterogeneous Cu–MnO catalyst for the direct functionalization of the C(sp)–H bond of the terminal alkynes with dialkyl phosphite under the base and additive-free conditions, in DMSO at 100 °C and in the presence of air as the sole oxidant. A control experiment with TEMPO or inert conditions indicates that the reactions do not proceed through a radical pathway and that oxygen is essential for these reactions. The protocol is compatible with a wide variety of functional groups and generates alkynylphosphonate in good to excellent yields (37–97%). The catalyst was recovered and reused up to five cycles without a significant loss of catalytic activity (from 95 to 85% yield) and with a negligible amount of Cu (<2 ppm) leached in the filtrate. The hot filtration test confirmed the heterogeneity of the reaction.

6. Carbon–Sulfur and Carbon–Selenium (C–S/C–Se) Bond Formation

Organochalcogenides (S, Se) have attracted considerable attention due to their wide range of applications as pharmaceuticals, building blocks and intermediates for the synthesis of functional materials [114,115]. Therefore, the catalytic activation of C–H bonds to form C–S/Se bonds has been studied in the last few years [116,117], but in this context, the use of metal and metal oxide nanoparticles is rare.

Alkynyl sulfides and selenides are extremely versatile intermediates in organic synthesis and can be obtained via the cross-coupling reaction of diaryl disulfide or diaryl diselenides with terminal alkynes by activating the C(sp)–H and S–S or Se–Se bonds (Scheme 31) [118–122].



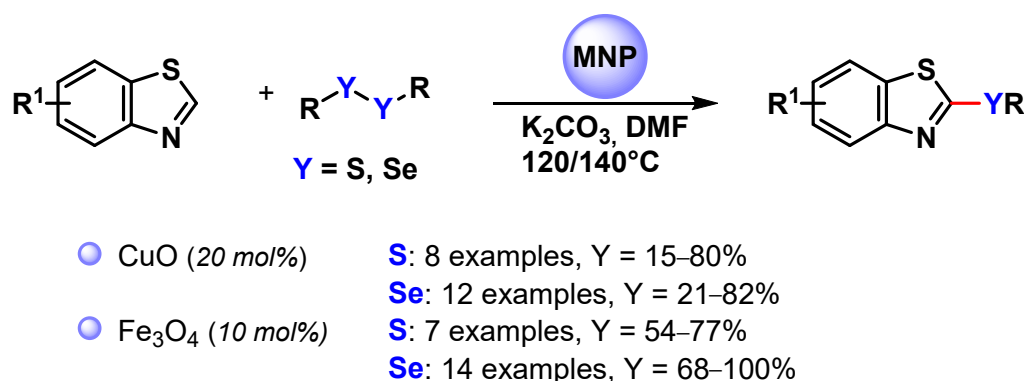
Scheme 31. Synthesis of alkynyl sulfides and selenides via direct C(sp)–H activation.

In 2015, Park and coworkers [118] employed Cu nanoparticles for the preparation of alkynyl disulfide via the C(sp)-H activation of alkynes in DMSO at 70 °C, using Na₂CO₃ as the base and an O₂ atmosphere. With this protocol, a wide range of alkynyl sulfides were synthesized using a low catalyst loading (0.5 mol% Cu). The same protocol was also extended to the preparation of an alkynyl selenide (R¹ = Ph, R = C₁₀H₂₁). The authors proposed a mechanism that involves the oxidative addition of Cu(0) to disulfide or diselenide, followed by the C(sp)-H activation of alkyne in the presence of base and O₂, which regenerated the disulfide or the diselenide, and successive reductive elimination (Scheme 31).

In 2016, the same authors reported the use of magnetite nanoparticles supported on charcoal (Fe₃O₄/C) for the preparation of alkynyl selenides through the activation of C(sp)-H and Se-Se bonds under air, in the presence of KO^tBu as a base and EtOH as a solvent at 80 °C [119]. The catalyst was efficiently recovered with a magnetic field and recycled up to five runs with a negligible loss of its catalytic activity (from 83 to 78% conversion). Similarly, Braga and coworkers used CuO nanoparticles [120] or Fe₃O₄ nanoparticles [121] as efficient and recoverable catalysts for the preparation of alkynyl selenides.

In 2020, Yang and coworkers [122] prepared ultrafine and highly dispersed Ni₂P nanoparticles (3.2 nm) on N,P-codoped carbon (Ni₂P@NPC-800) for the base- and ligand-free cross-dehydrogenative coupling of terminal alkynes and thiols using air as the sole oxidant under mild conditions (DMF, 50 °C). Alkynyl thioethers were obtained in good to high yields (52–97%) with good compatibility to a wide range of functional groups. N-dopants used as basic sites in carbon supports play a key role in facilitating the activation of terminal alkynes via hydrogen bonding interactions.

In 2013, Zeni and coworkers [123] employed CuO nanoparticles for the C(sp²)-H bond activation of benzothiazole and promote the reaction with diorganyl disulfides or diselenides to access 2-(organochalcogen)benzothiazoles (Scheme 32). The process was performed in DMF at 140 °C in the presence of K₂CO₃ as a base, which was crucial for the formation of the products, obtained in moderate to good yields. The proposed mechanism involved S-S or Se-Se bond activation via oxidative addition on the surface of metal, followed by the C-H activation of benzothiazole and reductive elimination.

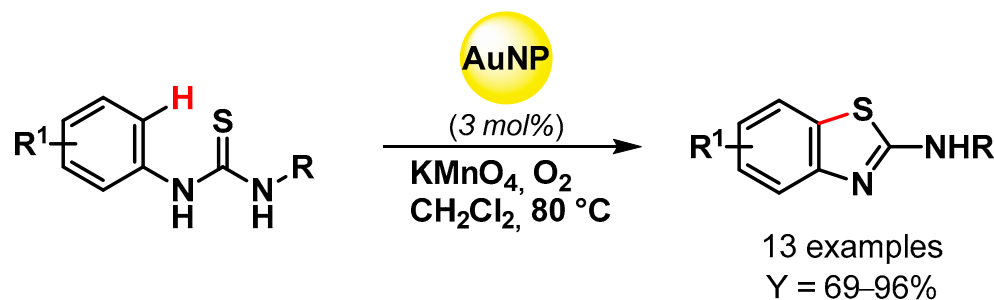


Scheme 32. Synthesis of 2-(organochalcogen)benzothiazoles via the direct C(sp²)-H activation of benzothiazoles.

A similar protocol was proposed by Braga and coworkers in 2018 [124] by using magnetically recoverable Fe₃O₄ nanoparticles (Scheme 32) [123,124]. Good to excellent yields were obtained for a large number of substrates, and the recovered catalyst maintained its activity and effectiveness for up to four runs (from 98 to 93% yield).

An efficient synthesis of 2-(N-substituted)aminobenzothiazoles via intramolecular C-S bond formation through Au-NPs catalyzed oxidative C-H bond activation was reported in 2015 by Gogoi and coworkers [125] (Scheme 33). Au nanoparticles with a size distribution between 1 and 20 nm were obtained from HAuCl₄ using *Kayea assamica* (sia nahor) aqueous fruit extract as the reducing and capping agent. The presence of KMnO₄ as cocatalyst

and an O₂ atmosphere allowed the obtention of 2-(N-substituted)aminobenzothiazoles with good to excellent yield. The catalyst was easily separated and reused for eight cycles without a noticeable loss of activity (from 90 to 81% yields).



Scheme 33. Synthesis of 2-(N-substituted)aminobenzothiazoles via intramolecular C–S bond formation.

7. Conclusions

To summarize this review article, we have reported that, in the literature, there are numerous examples wherein the direct activation/functionalization of an unreactive C–H bond could be promoted by metal or metal oxide nanoparticles to form new C–O and C–X (X = Cl, B, P, S and Se) bonds.

In the last decade, noble metals, such as palladium and gold nanoparticles or other platinum group metals (Ag, Pt, Rh, Ru, Ir), have undergone rapid development due to their high catalytic efficiency and possible recyclability. More recently, non-precious metal and metal oxide nanoparticles, mainly based on Cu, Fe and Ni, have been used for C–H bond activation as they show lower toxicity, being cheaper and possibly also more sustainable. In some cases, the use of visible-light irradiation can be also used to improve the performance of a nanocatalyst in the formation of new C–O bonds.

A key aspect of modern metal catalysis is linked to the recycling and separation of metal from the product. Regarding this concern, metal nanoparticles are very promising from a green perspective and for potential industrial applications. Their catalytic activity and recyclability can be improved through a good choice of support, which also can affect the size, distribution and stability of NPs. Moreover, the use of flow technology and/or an alternative energy source, such as microwave, light or ultrasound irradiation, can also influence the catalytic efficiency of metal NPs, opening up a large number of possible scenarios and intriguing applications.

The examples discussed in this review clearly prove that a careful design of metal nanoparticles is necessary, and it is very interesting in order to define highly active and selective catalytic systems for C–H activation processes, paving the way for more sustainable chemical production.

Author Contributions: Writing, review and editing, F.V., O.P. and L.V. All authors have read and agreed to the published version of the manuscript.

Funding: MUR: AMIS: “Dipartimenti di eccellenza—2018–2022”.

Acknowledgments: The Università degli Studi di Perugia and MUR are acknowledged for financial support to the project AMIS, through the program “Dipartimenti di Eccellenza—2018–2022”.

Conflicts of Interest: The authors declare no conflict of interest.

References

1. Dalton, T.; Faber, T.; Glorius, F. C–H Activation: Toward Sustainability and Applications. *ACS Cent. Sci.* **2021**, *7*, 245–261. [[CrossRef](#)] [[PubMed](#)]
2. Santoro, S.; Ferlin, F.; Vaccaro, L. *Sustainable Approaches to C–H Functionalizations Through Flow Techniques—Flow Chemistry*; RSC Green Chemistry: Cambridge, UK, 2020; pp. 199–216.

3. Santoro, S.; Ferlin, F.; Ackermann, L.; Vaccaro, L. C–H functionalization reactions under flow conditions. *Chem. Soc. Rev.* **2019**, *48*, 2767–2782. [[CrossRef](#)] [[PubMed](#)]
4. Santoro, S.; Marrocchi, A.; Lanari, D.; Ackermann, L.; Vaccaro, L. Towards Sustainable C–H Functionalization Reactions: The Emerging Role of Bio-Based Reaction Media. *Chem. Eur. J.* **2018**, *24*, 13383–13390. [[CrossRef](#)] [[PubMed](#)]
5. Ali, R.; Siddiqui, R. Recent Developments in Remote Meta-C–H Bond Functionalizations. *Adv. Synth. Catal.* **2021**, *363*, 1290–1316. [[CrossRef](#)]
6. Singh, P.; Chouhan, K.K.; Mukherjee, A. Ruthenium Catalyzed Intramolecular C–X (X=C, N, O, S) Bond Formation via C–H Functionalization: An Overview. *Chem. Asian J.* **2021**, *16*, 2392–2412. [[CrossRef](#)] [[PubMed](#)]
7. Dhawa, U.; Kaplaneris, N.; Ackermann, L. Green strategies for transition metal-catalyzed C–H activation in molecular syntheses. *Org. Chem. Front.* **2021**, *8*, 4886–4913. [[CrossRef](#)]
8. Rufino-Felipe, E.; Osorio-Yáñez, R.N.; Vera, M.; Valdés, H.; González-Sebastián, L.; Reyes-Sanchez, A.; Morales-Morales, D. Transition-metal complexes bearing chelating NHC Ligands. Catalytic activity in cross coupling reactions via C–H activation. *Polyhedron* **2021**, *204*, 115220. [[CrossRef](#)]
9. Zhang, Q.; Shi, B.-F. 2-(Pyridin-2-yl)isopropyl (PIP) Amine: An Enabling Directing Group for Divergent and Asymmetric Functionalization of Unactivated Methylene C(sp³)–H Bonds. *Acc. Chem. Res.* **2021**, *54*, 2750–2763. [[CrossRef](#)] [[PubMed](#)]
10. Zhang, M.; Wang, Q.; Peng, Y.; Chen, Z.; Wan, C.; Chen, J.; Zhao, Y.; Zhang, R.; Zhang, A.Q. Transition metal-catalyzed sp³ C–H activation and intramolecular C–N coupling to construct nitrogen heterocyclic scaffolds. *Chem. Commun.* **2019**, *55*, 13048–13065. [[CrossRef](#)]
11. Rouquet, G.; Chatani, N. Catalytic functionalization of C(sp²)–H and C(sp³)–H bonds by using bidentate directing groups. *Angew. Chem. Int. Ed.* **2013**, *52*, 11726–11743. [[CrossRef](#)]
12. Gandeepan, P.; Kaplaneris, N.; Santoro, S.; Vaccaro, L.; Ackermann, L. Biomass-Derived Solvents for Sustainable Transition Metal-Catalyzed C–H Activation. *ACS Sustainable Chem. Eng.* **2019**, *7*, 8023–8040. [[CrossRef](#)]
13. Gandeepan, P.; Muller, T.; Zell, D.; Cera, G.; Warratz, S.; Ackermann, L. 3d Transition Metals for C–H Activation. *Chem. Rev.* **2019**, *119*, 2192–2452. [[CrossRef](#)] [[PubMed](#)]
14. Chu, J.C.K.; Rovis, T. Complementary Strategies for Directed C(sp³)–H Functionalization: A Comparison of Transition-Metal-Catalyzed Activation, Hydrogen Atom Transfer, and Carbene/Nitrene Transfer. *Angew. Chem. Int. Ed.* **2018**, *57*, 62–101. [[CrossRef](#)] [[PubMed](#)]
15. Gandeepan, P.; Ackermann, L. Transient Directing Groups for Transformative C–H Activation by Synergistic Metal Catalysis. *Chem* **2018**, *4*, 199–222. [[CrossRef](#)]
16. Petrini, M. Regioselective Direct C–Alkenylation of Indoles. *Chem. Eur. J.* **2017**, *23*, 16115–16151. [[CrossRef](#)]
17. Arockiam, P.B.; Bruneau, C.; Dixneuf, P.H. Ruthenium(II)-Catalyzed C–H Bond Activation and Functionalization. *Chem. Rev.* **2012**, *112*, 5879–5918. [[CrossRef](#)]
18. Hashiguchi, B.G.; Bischof, S.M.; Konnick, M.M.; Periana, R.A. Designing Catalysts for Functionalization of Unactivated C–H Bonds Based on the CH Activation Reaction. *Acc. Chem. Res.* **2012**, *45*, 885–898. [[CrossRef](#)]
19. Shilov, A.E.; Shul’pin, G.B. Activation of C–H Bonds by Metal Complexes. *Chem. Rev.* **1997**, *97*, 2879–2932. [[CrossRef](#)]
20. Liu, B.; Romine, A.M.; Rubel, C.Z.; Engle, K.M.; Shi, B.-F. Transition-Metal-Catalyzed, Coordination-Assisted Functionalization of Nonactivated C(sp³)–H Bonds. *Chem. Rev.* **2021**, *121*, 14957–15074. [[CrossRef](#)]
21. Mandal, R.; Garai, B.; Sundararaju, B. Weak-Coordination in C–H Bond Functionalizations Catalyzed by 3d Metals. *ACS Catal.* **2022**, *12*, 3452–3506. [[CrossRef](#)]
22. Sági, A.; Rajkumar, T.; Kiss, J.; Kukovecz, Á.; Kónya, Z.; Somorjai, G.A. Metallic nanoparticles in heterogeneous catalysis. *Catal. Lett.* **2021**, *151*, 2153–2175. [[CrossRef](#)]
23. Valentini, F.; Ferlin, F.; Lilli, S.; Marrocchi, A.; Ping, L.; Gu, Y.; Vaccaro, L. Valorisation of urban waste to access low-cost heterogeneous palladium catalysts for cross-coupling reactions in biomass-derived γ -valerolactone. *Green Chem.* **2021**, *23*, 5887–5895. [[CrossRef](#)]
24. Trombettoni, V.; Ferlin, F.; Valentini, F.; Campana, F.; Silvetti, M.; Vaccaro, L. POLITAG-Pd (0) catalyzed continuous flow hydrogenation of lignin-derived phenolic compounds using sodium formate as a safe H-source. *Mol. Catal.* **2021**, *509*, 111613. [[CrossRef](#)]
25. Ohtaka, A. Recent Progress of Metal Nanoparticle Catalysts for C–C Bond Forming Reactions. *Catalysts* **2021**, *11*, 1266. [[CrossRef](#)]
26. Kumar, A.; Choudhary, P.; Kumar, A.; Camargo, P.H.; Krishnan, V. Recent advances in plasmonic photocatalysis based on TiO₂ and noble metal nanoparticles for energy conversion, environmental remediation, and organic synthesis. *Small* **2022**, *18*, 2101638. [[CrossRef](#)]
27. Ndolomingo, M.J.; Bingwa, N.; Meijboom, R. Review of supported metal nanoparticles: Synthesis methodologies, advantages and application as catalysts. *J. Mater. Sci.* **2020**, *55*, 6195–6241. [[CrossRef](#)]
28. Cortes-Clerget, M.; Akporji, N.; Takale, B.S.; Wood, A.; Landstrom, E.; Lipshutz, B.H. Earth-Abundant and Precious Metal Nanoparticle Catalysis. *Nanoparticles Catal.* **2020**, *77*–129. [[CrossRef](#)]
29. Hu, H.; Xin, J.H.; Hu, H.; Wang, X.; Miao, D.; Liu, Y. Synthesis and stabilization of metal nanocatalysts for reduction reactions—a review. *J. Mater. Chem. A* **2015**, *3*, 11157–11182. [[CrossRef](#)]
30. Tao, F.F. *Metal Nanoparticles for Catalysis: Advances and Applications*, 1st ed.; Royal Society of Chemistry: Cambridge, UK, 2014.

31. Valentini, F.; Piermatti, O.; Vaccaro, L. Metal nanoparticles as sustainable tools for C–N bond formation via C–H activation. *Molecules* **2021**, *26*, 4106. [[CrossRef](#)]
32. Baroliya, P.K.; Chopra, J.; Pal, T.; Maiti, S.; Al-Thabaiti, S.A.; Mokhtar, M.; Maiti, D. Supported Metal Nanoparticles Assisted Catalysis: A Broad Concept in Functionalization of Ubiquitous C–H Bonds. *ChemCatChem* **2021**, *13*, 4655–4678. [[CrossRef](#)]
33. Asensio, J.M.; Bouzouita, D.; van Leeuwen, P.W.N.M.; Chaudret, B. σ -H-H, σ -C–H, and σ -Si-H Bond Activation Catalyzed by Metal Nanoparticles. *Chem. Rev.* **2020**, *120*, 1042–1084. [[CrossRef](#)] [[PubMed](#)]
34. Valentini, F.; Brufani, G.; Latterini, L.; Vaccaro, L. Metal Nanoparticles Catalyzed C–C Bond Formation via C–H Activation. In *Advanced Heterogeneous Catalysts Volume 1: Applications at the Nano-Scale*; American Chemical Society: Washington, DC, USA, 2020; pp. 513–543. [[CrossRef](#)]
35. Saha, D.; Mukhopadhyay, C. Metal Nanoparticles: An Efficient Tool for Heterocycles Synthesis and Their Functionalization via C–H Activation. *Curr. Organocatal.* **2018**, *6*, 79–91. [[CrossRef](#)]
36. Pla, D.; Gómez, M. Metal and Metal Oxide Nanoparticles: A Lever for C–H Functionalization. *ACS Catal.* **2016**, *6*, 3537–3552. [[CrossRef](#)]
37. Ferlin, F.; Anastasiou, I.; Salameh, N.; Miyakoshi, T.; Baudoin, O.; Vaccaro, L. C(sp³)–H Arylation Promoted by a Heterogeneous Palladium-N-Heterocyclic Carbene Complex in Batch and Continuous Flow. *ChemSusChem* **2022**, *15*, e202102736. [[CrossRef](#)] [[PubMed](#)]
38. Salameh, N.; Anastasiou, I.; Ferlin, F.; Minio, F.; Chen, S.; Santoro, S.; Liu, P.; Gu, Y.; Vaccaro, L. Heterogeneous palladium-catalysed intramolecular C(sp³)–H α -arylation for the green synthesis of oxindoles. *Mol. Catal.* **2022**, *522*, 112211. [[CrossRef](#)]
39. Anastasiou, I.; Ferlin, F.; Viteritti, O.; Santoro, S.; Vaccaro, L. Pd/C-catalyzed aerobic oxidative C–H alkenylation of arenes in γ -valerolactone (GVL). *Mol. Catal.* **2021**, *513*, 111787. [[CrossRef](#)]
40. Ferlin, F.; Anastasiou, I.; Carpisassi, L.; Vaccaro, L. Aerobic waste-minimized Pd-catalysed C–H alkenylation in GVL using a tube-in-tube heterogeneous flow reactor. *Green Chem.* **2021**, *23*, 6576–6582. [[CrossRef](#)]
41. Campana, F.; Massaccesi, B.M.; Santoro, S.; Piermatti, O.; Vaccaro, L. Polarclean/Water as a Safe and Recoverable Medium for Selective C2-Arylation of Indoles Catalyzed by Pd/C. *ACS Sust. Chem. Eng.* **2020**, *8*, 16441–16450. [[CrossRef](#)]
42. Sciosci, D.; Valentini, F.; Ferlin, F.; Chen, S.; Gu, Y.; Piermatti, O.; Vaccaro, L. A heterogeneous and recoverable palladium catalyst to access the regioselective C–H alkenylation of quinoline N-oxides. *Green Chem.* **2020**, *22*, 6560–6566. [[CrossRef](#)]
43. Ferlin, F.; Luque Navarro, P.M.; Gu, Y.; Lanari, D.; Vaccaro, L. Waste minimized synthesis of pharmaceutically active compounds via heterogeneous manganese catalysed C–H oxidation in flow. *Green Chem.* **2020**, *22*, 397–403. [[CrossRef](#)]
44. Ferlin, F.; van der Hulst, M.K.; Santoro, S.; Lanari, D.; Vaccaro, L. Continuous flow/waste minimized synthesis of benzoxazoles catalysed by heterogeneous manganese systems. *Green Chem.* **2019**, *21*, 5298–5305. [[CrossRef](#)]
45. Paul, A.; Chatterjee, D.; Banerjee, S.; Somnath Yadav, S. Synthesis of 3-alkenylindoles through regioselective C–H alkenylation of indoles by a ruthenium nanocatalyst. *Beilstein J. Org. Chem.* **2020**, *16*, 140–148. [[CrossRef](#)] [[PubMed](#)]
46. Bora, P.; Konwar, D.; Dewan, A.; Das, M.R.; Bora, U. Bio-carbon-layered CuO-catalyzed decarboxylative alkenylation of cyclic ethers. *New J. Chem.* **2022**, *46*, 12551–12557. [[CrossRef](#)]
47. Xie, R.; Xie, F.; Zhou, C.J.; Jiang, H.F.; Zhang, M. Hydrogen transfer-mediated selective dual C–H alkylations of 2-alkylquinolines by doped TiO₂-supported nanocobalt oxides. *J. Catal.* **2019**, *377*, 449–454. [[CrossRef](#)]
48. Abeadi, N.; Zhiani, R.; Motavalizadehkakhky, A.; Omidvar, M.; Hosseiny, M.S. FPS/[Fe(Bpy)₃]²⁺ NPs as a nanocatalyst for production of quinoline-2-ones through the annulation of ortho-heteroaryl anilines and CO₂. *Inorg. Chem. Commun.* **2021**, *123*, 108356. [[CrossRef](#)]
49. Rana, P.; Gaur, R.; Kaushik, B.; Rana, P.; Yadav, S.; Yadav, P.; Sharma, P.; Gawande, M.B.; Sharma, R.K. Surface engineered Iridium-based magnetic photocatalyst paving a path towards visible light driven C–H arylation and cyanation reaction. *J. Catal.* **2021**, *401*, 297–308. [[CrossRef](#)]
50. Rana, P.; Gaur, R.; Gupta, R.; Arora, G.; Jayashree, A.; Sharma, R.K. Cross-dehydrogenative C(sp³)–C(sp³) coupling via C–H activation using magnetically retrievable ruthenium-based photoredox nanocatalyst under aerobic conditions. *Chem. Commun.* **2019**, *55*, 7402–7405. [[CrossRef](#)]
51. Gruttadauria, M.; Giacalone, F.; Noto, R. “Release and catch” catalytic systems. *Green Chem.* **2013**, *15*, 2608–2618. [[CrossRef](#)]
52. Fairlamb, I.J.S.; Lee, A.F. Fundamental Pd(0)/Pd(II) redox steps in cross-coupling reactions: Homogeneous, hybrid homogeneous–heterogeneous to heterogeneous mechanistic pathways for C–C couplings. In *Catalytic C–H/C–X Bond Functionalization: Transition Metal Mediation*; RSC Catalysis Series; No. 11; Ribas, X., Ed.; RSC Publishing: Cambridge, UK, 2013; pp. 72–107.
53. Fessner, N.D. P450 Monooxygenases Enable Rapid Late-Stage Diversification of Natural Products via C–H Bond Activation. *ChemCatChem* **2019**, *11*, 2226–2242. [[CrossRef](#)]
54. Borpatra, P.J.; Deka, B.; Deb, M.L.; Baruah, P.K. Recent advances in intramolecular C–O/C–N/C–S bond formation: Via C–H functionalization. *Org. Chem. Front.* **2019**, *6*, 3445–3489. [[CrossRef](#)]
55. Newhouse, T.; Baran, P.S. If C–H Bonds Could Talk: Selective C–H Bond Oxidation. *Angew. Chem. Int. Ed.* **2011**, *50*, 3362–3374. [[CrossRef](#)] [[PubMed](#)]
56. Schuchardt, U.; Cardoso, D.; Sercheli, R.; Pereira, R.; da Cruz, R.S.; Guerreiro, M.C.; Mandelli, D.; Spinace, E.V.; Pires, E.L. Cyclohexane oxidation continues to be a challenge. *Appl. Catal. A Gen.* **2001**, *211*, 1–17. [[CrossRef](#)]
57. Dimitratos, N.; Lopez-Sanchez, J.A.; Hutchings, G.J. Selective liquid phase oxidation with supported metal nanoparticles. *Chem. Sci.* **2012**, *3*, 20–44. [[CrossRef](#)]

58. Wang, V.C.-C.; Maji, S.; Chen, P.P.-Y.; Lee, H.K.; Yu, S.S.-F.; Chan, S.I. Alkane Oxidation: Methane Monooxygenases, Related Enzymes, and Their Biomimetics. *Chem. Rev.* **2017**, *117*, 8574–8621. [[CrossRef](#)] [[PubMed](#)]
59. Latimer, A.A.; Kulkarni, A.R.; Aljama, H.; Montoya, J.H.; Yoo, J.S.; Tsai, C.; Abild-Pedersen, F.; Studt, F.; Noerskov, J.K. Understanding trends in C–H bond activation in heterogeneous catalysis. *Nat. Mater.* **2017**, *16*, 225–229. [[CrossRef](#)]
60. Freakley, S.J.; Dimitratos, N.; Willock, D.J.; Taylor, S.H.; Kiely, C.J.; Hutchings, G.J. Methane Oxidation to Methanol in Water. *Acc. Chem. Res.* **2021**, *54*, 2614–2623. [[CrossRef](#)]
61. Sundberg, M.R.; Zborowski, K.K.; Alkorta, I. Multiple 3cA2e bonding of methane with metal cations. *Chem. Phys. Lett.* **2011**, *515*, 210–213. [[CrossRef](#)]
62. Voutchkova, A.M.; Crabtree, R.H. Iridium-catalyzed benzylic C–H activation and functionalization of alkyl arenes. *J. Mol. Catal. A Chem.* **2009**, *312*, 1–6. [[CrossRef](#)]
63. Kesavan, L.; Tiruvalam, R.; Ab Rahim, M.H.; bin Saiman, M.I.; Enache, D.I.; Jenkins, R.L.; Dimitratos, N.; Lopez-Sanchez, J.A.; Taylor, S.H.; Knight, D.W.; et al. Solvent-Free Oxidation of Primary Carbon-Hydrogen Bonds in Toluene Using Au-Pd Alloy Nanoparticles. *Science* **2011**, *331*, 195–199. [[CrossRef](#)]
64. Binsaiman, M.I.; Brett, G.L.; Tiruvalam, R.; Forde, M.M.; Sharples, K.; Thetford, A.; Jenkins, R.L.; Dimitratos, N.; Lopez-Sanchez, J.A.; Murphy, D.M.; et al. Involvement of surface-bound radicals in the oxidation of toluene using supported Au-Pd nanoparticles. *Angew. Chem. Int. Ed.* **2012**, *51*, 5981–5985. [[CrossRef](#)]
65. Lingampalli, S.R.; Gupta, U.; Gautam, U.K.; Rao, C.N.R. Oxidation of toluene and other examples of C–H bond activation by CdO₂ and ZnO₂ nanoparticles. *ChemPlusChem* **2013**, *78*, 837–842. [[CrossRef](#)] [[PubMed](#)]
66. Das, P.P.; Chowdhury, B. Indium oxide nanoparticles embedded in TUD-1 as a highly selective catalyst for toluene to benzaldehyde oxidation using TBHP as oxidant. *Chem. Pap.* **2020**, *74*, 2091–2100. [[CrossRef](#)]
67. Biswas, R.; Das, S.K.; Bhaduri, S.N.; Bhaumik, A.; Biswas, P. AgNPs Immobilized over Functionalized 2D Hexagonal SBA-15 for Catalytic C–H Oxidation of Hydrocarbons with Molecular Oxygen under Solvent-Free Conditions. *ACS Sust. Chem. Eng.* **2020**, *8*, 5856–5867. [[CrossRef](#)]
68. Dai, Y.; Poidevin, C.; Ochoa-Hernández, C.; Auer, A.A.; Tüysüz, H. A Supported Bismuth Halide Perovskite Photocatalyst for Selective Aliphatic and Aromatic C–H Bond Activation. *Angew. Chem. Int. Ed.* **2020**, *59*, 5788–5796. [[CrossRef](#)]
69. Zhang, Z.; Yang, Y.; Wang, Y.; Yang, L.; Li, Q.; Chen, L.; Xu, D. Revealing the A-Site Effect of Lead-Free A₃Sb₂Br₉ Perovskite in Photocatalytic C(sp³)–H Bond Activation. *Angew. Chem. Int. Ed.* **2020**, *59*, 18136–18139. [[CrossRef](#)] [[PubMed](#)]
70. Yan, Y.; Ye, B.; Chen, M.; Lu, L.; Yu, J.; Zhou, Y.; Wang, Y.; Liu, J.; Xiao, L.; Zou, S.; et al. Site-specific deposition creates electron-rich Pd atoms for unprecedented C–H activation in aerobic alcohol oxidation. *Chin. J. Catal.* **2020**, *41*, 1240–1247. [[CrossRef](#)]
71. Majumdar, B.; Bhattacharya, T.; Sarma, T.K. Gold Nanoparticle-Polydopamine-Reduced Graphene Oxide Ternary Nanocomposite as an Efficient Catalyst for Selective Oxidation of Benzylic C(sp³)–H Bonds under Mild Conditions. *ChemCatChem* **2016**, *8*, 1825–1835. [[CrossRef](#)]
72. Huang, C.; Su, X.; Gu, X.; Liu, R.; Zhu, H. Bimetallic oxide nanoparticles confined in ZIF-67-derived carbon for highly selective oxidation of saturated C–H bond in alkyl arenes. *Appl. Organomet. Chem.* **2021**, *35*, e6047. [[CrossRef](#)]
73. Dong, Z.; Pan, H.; Yang, L.; Fan, L.; Xiao, Y.; Chen, J.; Wang, W. Porous organic polymer immobilized copper nanoparticles as heterogeneous catalyst for efficient benzylic C–H bond oxidation. *J. Saudi Chem. Soc.* **2022**, *26*, 101397. [[CrossRef](#)]
74. Liu, H.; Chen, G.; Jiang, H.; Li, Y.; Luque, R. From alkyl aromatics to aromatic esters: Efficient and selective C–H activation promoted by a bimetallic heterogeneous catalyst. *ChemSusChem* **2012**, *5*, 1892–1896. [[CrossRef](#)]
75. Verma, S.; Nasir Baig, R.B.; Nadagouda, M.N.; Varma, R.S. Photocatalytic C–H activation and oxidative esterification using Pd@g-C₃N₄. *Catal. Today* **2018**, *309*, 248–252. [[CrossRef](#)] [[PubMed](#)]
76. Zhang, Y.; Liu, G. Development of highly efficient and durable reduced graphene oxide decorated with Ag/Co₃O₄ nanocomposite towards photocatalytic C–H activation. *J. Photochem. Photobiol. A Chem* **2020**, *394*, 112494. [[CrossRef](#)]
77. Zhang, B.; Yang, X.; Li, J.; Cheng, G. Selective aerobic oxidation of alkyl aromatics on Bi₂MoO₆ nanoplates decorated with Pt nanoparticles under visible light irradiation. *Chem. Commun.* **2018**, *54*, 12194–12197. [[CrossRef](#)] [[PubMed](#)]
78. Gupta, S.S.R.; Lakshmi Kantam, M. Finely dispersed CuO on nitrogen-doped carbon hollow nanospheres for selective oxidation of sp³ C–H bonds. *New J. Chem.* **2021**, *45*, 16179–16186. [[CrossRef](#)]
79. Sahin, Y.; Sika-Nartey, A.T.; Ercan, K.E.; Kocak, Y.; Senol, S.; Ozensoy, E.; Türkmen, Y.E. Precious Metal-Free LaMnO₃ Perovskite Catalyst with an Optimized Nanostructure for Aerobic C–H Bond Activation Reactions: Alkylarene Oxidation and Naphthol Dimerization. *ACS Appl. Mater. Interfaces* **2021**, *13*, 5099–5110. [[CrossRef](#)]
80. Hayashi, E.; Tamura, T.; Aihara, T.; Kamata, K.; Hara, M. Base-Assisted Aerobic C–H Oxidation of Alkylarenes with a Murdochite-Type Oxide Mg₆MnO₈ Nanoparticle Catalyst. *ACS Appl. Mater. Interfaces* **2022**, *14*, 6528–6537. [[CrossRef](#)]
81. Korwar, S.; Brinkley, K.; Siamaki, A.R.; Gupton, B.F.; Ellis, K.C. Selective N-Chelation-directed C–H activation reactions catalyzed by Pd(II) nanoparticles supported on multiwalled carbon nanotubes. *Org. Lett.* **2015**, *17*, 1782–1785. [[CrossRef](#)]
82. Wang, F.; Huang, F.; Yu, Y.; Zhou, S.; Wang, Z.; Zhang, W. Monodisperse CuPd alloy nanoparticles supported on reduced graphene oxide as efficient catalyst for directed C–H activation. *Catal. Commun.* **2021**, *153*, 106296. [[CrossRef](#)]
83. Mendez, V.; Guillois, K.; Daniele, S.; Tuel, A.; Caps, V. Aerobic methylcyclohexane-promoted epoxidation of stilbene over gold nanoparticles supported on Gd-doped titania. *Dalton Trans.* **2010**, *39*, 8457–8463. [[CrossRef](#)]
84. Liu, Y.; Tsunoyama, H.; Akita, T.; Xie, S.; Tsukuda, T. Aerobic oxidation of cyclohexane catalyzed by size-controlled Au clusters on hydroxyapatite: Size effect in the sub-2 nm regime. *ACS Catal.* **2011**, *1*, 2–6. [[CrossRef](#)]

85. Long, J.; Liu, H.; Wu, S.; Liao, S.; Li, Y. Selective oxidation of saturated hydrocarbons using Au-Pd alloy nanoparticles supported on metal-organic frameworks. *ACS Catal.* **2013**, *3*, 647–654. [[CrossRef](#)]
86. Liu, R.; Huang, H.; Li, H.; Liu, Y.; Zhong, J.; Li, Y.; Zhang, S.; Kang, Z. Metal nanoparticle/carbon quantum dot composite as a photocatalyst for high-efficiency cyclohexane oxidation. *ACS Catal.* **2014**, *4*, 328–336. [[CrossRef](#)]
87. Donoeva, B.G.; Ovoshchnikov, D.S.; Golovko, V.B. Establishing a Au nanoparticle size effect in the oxidation of cyclohexene using gradually changing Au catalysts. *ACS Catal.* **2013**, *3*, 2986–2991. [[CrossRef](#)]
88. Priyadarshini, S.; Amal Joseph, P.J.; Lakshmi Kantam, M. Copper catalyzed cross-coupling reactions of carboxylic acids: An expedient route to amides, 5-substituted γ -lactams and α -acyloxy esters. *RSC Adv.* **2013**, *3*, 18283–18287. [[CrossRef](#)]
89. Bao, U.; Muschin, T.; Bao, A.; Bao, Y.S.; Jia, M. FeNP-loaded coal-bearing kaolin catalysts for the direct esterification of benzoic acid with cyclic ether via C(sp³)-H bond activation. *Green Chem. Lett. Rev.* **2021**, *14*, 565–577. [[CrossRef](#)]
90. Tian, K.; Liu, W.J.; Zhang, S.; Jiang, H. One-pot synthesis of a carbon supported bimetallic Cu-Ag NPs catalyst for robust catalytic hydroxylation of benzene to phenol by fast pyrolysis of biomass waste. *Green Chem.* **2016**, *18*, 5643–5650. [[CrossRef](#)]
91. Verma, S.; Nasir Baig, R.B.; Nadagouda, M.N.; Varma, R.S. Hydroxylation of Benzene via C-H Activation Using Bimetallic CuAg@g-C₃N₄. *ACS Sust. Chem. Eng.* **2017**, *5*, 3637–3640. [[CrossRef](#)]
92. Losada-García, N.; Rodríguez-Otero, A.; Palomo, J.M. Tailorable synthesis of heterogeneous enzyme-copper nanobiohybrids and their application in the selective oxidation of benzene to phenol. *Catal. Sci. Technol.* **2020**, *10*, 196–206. [[CrossRef](#)]
93. Zhang, Y.; Zhao, Y.; Luo, Y.; Xiao, L.; Huang, Y.; Li, X.; Peng, Q.; Liu, Y.; Yang, B.; Zhu, C.; et al. Directed Aromatic C-H Activation/Acetoxylation Catalyzed by Pd Nanoparticles Supported on Graphene Oxide. *Org. Lett.* **2017**, *19*, 6470–6473. [[CrossRef](#)]
94. Mondal, J.; Borah, P.; Sreejith, S.; Nguyen, K.T.; Han, X.; Ma, X.; Zhao, Y. Morphology-tuned exceptional catalytic activity of porous-polymer-supported Mn₃O₄ in aerobic sp³ C-H bond oxidation of aromatic hydrocarbons and alcohols. *ChemCatChem* **2014**, *6*, 3518–3529. [[CrossRef](#)]
95. Salarinejad, N.; Dabiri, M.; Movahed, S.K. Directed aromatic C-H functionalization of N-arylcarbamates and quinazolinones catalyzed by palladium nanoparticles supported on nitrogen-doped graphene. *Colloids Interface Sci. Commun.* **2022**, *47*, 100606. [[CrossRef](#)]
96. Payra, S.; Saha, A.; Guchhait, S.; Banerjee, S. Direct CuO nanoparticle-catalyzed synthesis of poly-substituted furans: Via oxidative C-H/C-H functionalization in aqueous medium. *RSC Adv.* **2016**, *6*, 33462–33467. [[CrossRef](#)]
97. Yatabe, T.; Jin, X.; Mizuno, N.; Yamaguchi, K. Unusual Olefinic C-H Functionalization of Simple Chalcones toward Aurones Enabled by the Rational Design of a Function-Integrated Heterogeneous Catalyst. *ACS Catal.* **2018**, *8*, 4969–4978. [[CrossRef](#)]
98. Jayarajan, R.; Kumar, R.; Gupta, J.; Dev, G.; Kadu, P.; Chatterjee, D.; Bahadur, D.; Maiti, D.; Maji, S.K. Fabrication of an amyloid fibril-palladium nanocomposite: A sustainable catalyst for C-H activation and the electrooxidation of ethanol. *J. Mater. Chem. A* **2019**, *7*, 4486–4493. [[CrossRef](#)]
99. Murty, M.S.R.; Penthala, R.; Buddana, S.K.; Prakasham, R.S.; Das, P.; Polepalli, S.; Jain, N.; Bojja, S. Recyclable CuO nanoparticles-catalyzed synthesis of novel-2,5-disubstituted 1,3,4-oxadiazoles as antiproliferative, antibacterial, and antifungal agents. *Med. Chem. Res.* **2014**, *23*, 4579–4594. [[CrossRef](#)]
100. Saberi, D.; Mansoori, S.; Ghaderi, E.; Niknam, K. Copper nanoparticles on charcoal: An effective nanocatalyst for the synthesis of enol carbamates and amides via an oxidative coupling route. *Tetrahedron. Lett.* **2016**, *57*, 95–99. [[CrossRef](#)]
101. Vishwakarma, R.; Gadipelly, C.; Nakhate, A.; Deshmukh, G.; Mannepalli, L.K. Copper supported Mg-Al hydrotalcite derived oxide catalyst for enol carbamates synthesis via C-H bond activation of formamides. *Catal. Commun.* **2020**, *147*, 106150. [[CrossRef](#)]
102. Kim, K.; Jung, Y.; Lee, S.; Kim, M.; Shin, D.; Byun, H.; Cho, S.J.; Song, H.; Kim, H. Directed C-H Activation and Tandem Cross-Coupling Reactions Using Palladium Nanocatalysts with Controlled Oxidation. *Angew. Chem. Int. Ed.* **2017**, *56*, 6952–6956. [[CrossRef](#)]
103. Pascanu, V.; Carson, F.; Solano, M.V.; Su, J.; Zou, X.; Johansson, M.J.; Martín-Matute, B. Selective Heterogeneous C-H Activation/Halogenation Reactions Catalyzed by Pd@MOF Nanocomposites. *Chem. Eur. J.* **2016**, *22*, 3729–3737. [[CrossRef](#)]
104. Warratz, S.; Burns, D.J.; Zhu, C.; Korvorapun, K.; Rogge, T.; Scholz, J.; Jooss, C.; Gelman, D.; Ackermann, L. meta -C-H Bromination on Purine Bases by Heterogeneous Ruthenium Catalysis. *Angew. Chem. Int. Ed.* **2017**, *56*, 1557–1560. [[CrossRef](#)]
105. Mkhallid, I.A.I.; Barnard, J.H.; Marder, T.B.; Murphy, J.M.; Hartwig, J.F. C-H activation for the construction of C-B bonds. *Chem. Rev.* **2010**, *110*, 890–931. [[CrossRef](#)] [[PubMed](#)]
106. Ishiyama, T.; Ishida, K.; Takagi, J.; Miyaura, N. Palladium-Catalyzed Benzylic C-H Borylation of Alkylbenzenes with Bis(pinacolato)diboron or Pinacolborane. *Chem. Lett.* **2001**, *30*, 1082–1083. [[CrossRef](#)]
107. Yinghuai, Z.; Chenyan, K.; Ang, T.P.; Emi, A.; Monalisa, W.; Louis, L.K.J.; Hosmane, N.S.; Maguire, J.A. Catalytic phenylborylation reaction by iridium(0) nanoparticles produced from hydrido-iridium carborane. *Inorg. Chem.* **2008**, *47*, 5756–5761. [[CrossRef](#)] [[PubMed](#)]
108. Yan, G.; Jiang, Y.; Kuang, C.; Wang, S.; Liu, H.; Zhang, Y.; Wang, J. Nano-Fe₂O₃-catalyzed direct borylation of arenes. *Chem. Commun.* **2010**, *46*, 3170–3172. [[CrossRef](#)]
109. Das, A.; Hota, P.K.; Mandal, S.K. Nickel-Catalyzed C(sp²)-H Borylation of Arenes. *Organometallics* **2019**, *38*, 3286–3293. [[CrossRef](#)]
110. Demmer, C.S.; Krogsgaard-Larsen, N.; Bunch, L. Review on modern advances of chemical methods for the introduction of a phosphonic acid group. *Chem. Rev.* **2011**, *111*, 7981–8006. [[CrossRef](#)]

111. Moglie, Y.; Mascaró, E.; Gutierrez, V.; Alonso, F.; Radivoy, G. Base-Free Direct Synthesis of Alkynylphosphonates from Alkynes and H-Phosphonates Catalyzed by Cu₂O. *J. Org. Chem.* **2016**, *81*, 1813–1818. [[CrossRef](#)]
112. Yuan, T.; Chen, F.; Lu, G.-P. Direct synthesis of alkynylphosphonates from alkynes and phosphite esters catalyzed by Cu/Cu₂O nanoparticles supported on Nb₂O₅. *New J. Chem.* **2018**, *42*, 13957–13962. [[CrossRef](#)]
113. Singh, H.; Sahoo, T.; Sen, C.; Galani, S.M.; Ghosh, S.C. Aerobic oxidative alkynylation of H-phosphonates and amides: An efficient route for the synthesis of alkynylphosphonates and ynamides using a recyclable Cu-MnO catalyst. *Catal. Sci. Technol.* **2019**, *9*, 1691–1698. [[CrossRef](#)]
114. Tabarelli, G.; Dornelles, L.; Iglesias, B.A.; Gonçalves, D.F.; Terra Stefanello, S.; Soares, F.A.A.; Piccoli, B.C.; D'Avila da Silva, F.; da Rocha, J.B.T.; Schultze, E.; et al. Synthesis and Antitumoral Lung Carcinoma A549 and Antioxidant Activity Assays of New Chiral β -Aryl-Chalcogenium Azide Compounds. *ChemistrySelect* **2017**, *2*, 8423–8430. [[CrossRef](#)]
115. Brutchey, R.L. Diorganyl Dichalcogenides as Useful Synthons for Colloidal Semiconductor Nanocrystals. *Acc. Chem. Res.* **2015**, *48*, 2918–2926. [[CrossRef](#)]
116. Shen, C.; Zhang, P.; Sun, Q.; Bai, S.; Hor, T.S.A.; Liu, X. Recent advances in C–S bond formation via C–H bond functionalization and decarboxylation. *Chem. Soc. Rev.* **2015**, *44*, 291–314. [[CrossRef](#)] [[PubMed](#)]
117. Iwasaki, M.; Nishihara, Y. Palladium-catalysed direct thiolation and selenation of aryl C–H bonds assisted by directing groups. *Dalton Trans.* **2016**, *45*, 15278–15284. [[CrossRef](#)] [[PubMed](#)]
118. Mohan, B.; Hwang, S.; Woo, H.; Park, K.H. Copper Nanoparticle Catalyzed Formation of C–S Bonds through Activation of S–S and C–H Bonds: An Easy Route to Alkynyl Sulfides. *Synthesis* **2015**, *47*, 3741–3745. [[CrossRef](#)]
119. Mohan, B.; Park, J.C.; Park, K.H. Mechanochemical Synthesis of Active Magnetite Nanoparticles Supported on Charcoal for Facile Synthesis of Alkynyl Selenides by C–H Activation. *ChemCatChem* **2016**, *8*, 2345–2350. [[CrossRef](#)]
120. Godoi, M.; Ricardo, E.W.; Frizon, T.E.; Rocha, M.S.T.; Singh, D.; Paixão, M.W.; Braga, A.L. An efficient synthesis of alkynyl selenides and tellurides from terminal acetylenes and diorganyl diselenides or ditellurides catalyzed by recyclable copper oxide nanopowder. *Tetrahedron* **2012**, *68*, 10426–10430. [[CrossRef](#)]
121. Godoi, M.; Liz, D.G.; Ricardo, E.W.; Rocha, M.S.T.; Azeredo, J.B.; Braga, A.L. Magnetite (Fe₃O₄) nanoparticles: An efficient and recoverable catalyst for the synthesis of alkynyl chalcogenides (selenides and tellurides) from terminal acetylenes and diorganyl dichalcogenides. *Tetrahedron* **2014**, *70*, 3349–3354. [[CrossRef](#)]
122. Song, T.; Ren, P.; Xiao, J.; Yuan, Y.; Yang, Y. Highly dispersed Ni₂P nanoparticles on N,P-codoped carbon for efficient cross-dehydrogenative coupling to access alkynyl thioethers. *Green Chem.* **2020**, *22*, 651–656. [[CrossRef](#)]
123. Rosario, A.R.; Casola, K.K.; Oliveira, C.E.S.; Zeni, G. Copper oxide nanoparticle-catalyzed chalcogenation of the carbon-hydrogen bond in thiazoles: Synthesis of 2-(organochalcogen) thiazoles. *Adv. Synth. Catal.* **2013**, *355*, 2960–2966. [[CrossRef](#)]
124. Rafique, J.; Saba, S.; Frizon, T.E.A.; Braga, A.L. Fe₃O₄ nanoparticles: A robust and magnetically recoverable catalyst for direct C–H bond selenylation and sulfenylation of benzothiazoles. *ChemistrySelect* **2018**, *3*, 328–334. [[CrossRef](#)]
125. Gogoi, P.; Paul, B.; Hazarika, S.; Barman, P. Gold nanoparticle catalyzed intramolecular C–S bond formation/C–H bond functionalization/cyclization cascades. *RSC Adv.* **2015**, *5*, 57433–57436. [[CrossRef](#)]

Disclaimer/Publisher's Note: The statements, opinions and data contained in all publications are solely those of the individual author(s) and contributor(s) and not of MDPI and/or the editor(s). MDPI and/or the editor(s) disclaim responsibility for any injury to people or property resulting from any ideas, methods, instructions or products referred to in the content.